Cell Reports

Article

# A salivary gland-secreted peptide regulates insect systemic growth

## Graphical abstract

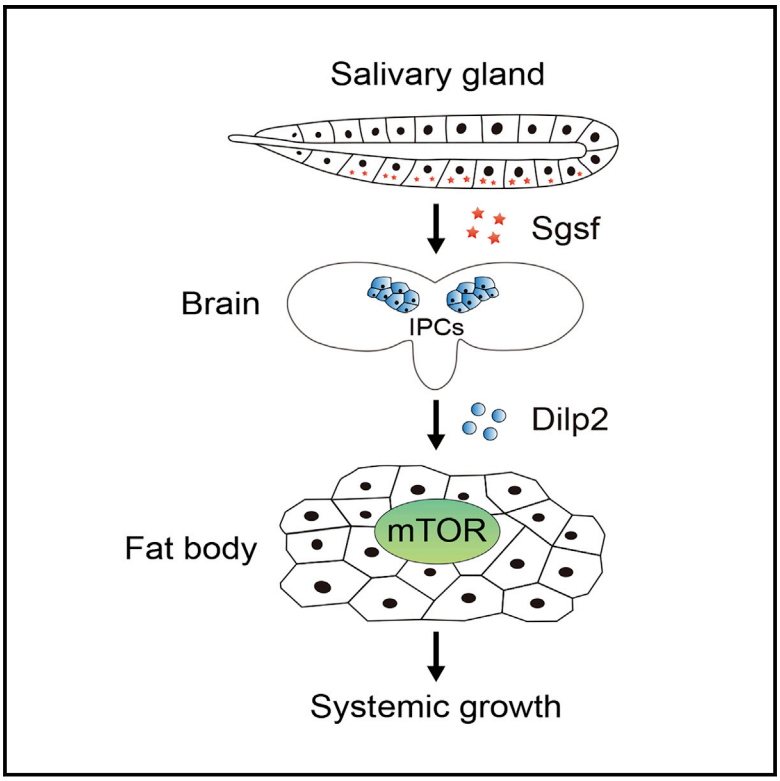


## Highlights

- Salivary gland ablation retards systemic growth in *Drosophila*
- Salivary gland-derived Sgsf peptide can be secreted into the hemolymph
- *Sgsf* knockout phenocopies the effects of salivary gland ablation on systemic growth
- Sgsf regulates Dilp2 secretion from brain IPCs and IIS/mTOR signaling in the fat body

## Authors

Zheng Li, Wenliang Qian, Wei Song, ..., Norbert Perrimon, Qingyou Xia, Daojun Cheng

## Correspondence

chengdj@swu.edu.cn (D.C.), xiaqy@swu.edu.cn (Q.X.), perrimon@genetics.med.harvard.edu (N.P.)

## In brief

Li et al. characterize an endocrine function for *Drosophila* salivary gland in promoting larval systemic growth by secreting Sgsf peptide into the hemolymph to modulate IIS/mTOR signaling

Li et al., 2022, Cell Reports *38*, 110397
February 22, 2022 
https://doi.org/10.1016/j.celrep.2022.110397

CellPress

Cell Reports

CellPress
OPEN ACCESS

Article

# A salivary gland-secreted peptide regulates insect systemic growth

Zheng Li,[1,2,7] Wenliang Qian,[1,2,7] Wei Song,[3,4] Tujing Zhao,[1,2] Yan Yang,[1,2] Weina Wang,[1,2] Ling Wei,[5] Dongchao Zhao,[1,2] Yaoyao Li,[1,2] Norbert Perrimon,[4,6,*] Qingyou Xia,[1,2,*] and Daojun Cheng[1,2,8,*]

[1]State Key Laboratory of Silkworm Genome Biology, Biological Science Research Center, Southwest University, Chongqing 400715, China
[2]Chongqing Key Laboratory of Sericultural Science, Southwest University, Chongqing 400715, China
[3]Medical Research Institute, Wuhan University, Wuhan 430071, China
[4]Department of Genetics, Blavatnik Institute, Harvard Medical School, Boston, MA 02115, USA
[5]School of Life Sciences, Southwest University, Chongqing 400715, China
[6]Howard Hughes Medical Institute, Boston, MA 02115, USA
[7]These authors contributed equally
[8]Lead contact
*Correspondence: chengdj@swu.edu.cn (D.C.), xiaqy@swu.edu.cn (Q.X.), perrimon@genetics.med.harvard.edu (N.P.)
https://doi.org/10.1016/j.celrep.2022.110397

## SUMMARY

Insect salivary glands have been previously shown to function in pupal attachment and food lubrication by secreting factors into the lumen via an exocrine way. Here, we find in *Drosophila* that a salivary gland-derived secreted factor (Sgsf) peptide regulates systemic growth via an endocrine way. Sgsf is specifically expressed in salivary glands and secreted into the hemolymph. *Sgsf* knockout or salivary gland-specific *Sgsf* knockdown decrease the size of both the body and organs, phenocopying the effects of genetic ablation of salivary glands, while salivary gland-specific *Sgsf* overexpression increases their size. Sgsf promotes systemic growth by modulating the secretion of the insulin-like peptide Dilp2 from the brain insulin-producing cells (IPCs) and affecting mechanistic target of rapamycin (mTOR) signaling in the fat body. Altogether, our study demonstrates that Sgsf mediates the roles of salivary glands in *Drosophila* systemic growth, establishing an endocrine function of salivary glands.

## INTRODUCTION

Insect salivary glands generally consist of a common duct that connects to the mouth and two individual lateral ducts, each of which connects to a gland composed of columnar epithelial secretory cells surrounding a lumen (Abrams et al., 2003; Pirraglia and Myat, 2010). Extensive studies in *Drosophila* have shown that the salivary glands develop from embryonic epithelial placodes and are specified following several rounds of mitosis during the embryonic period (Abrams et al., 2003; Bradley et al., 2001; Camelo and Luschnig, 2021). The rapid growth of salivary glands is achieved by an endocycle-induced increase in cell size during the larval period (Edgar et al., 2014; Zielke et al., 2013), scaling with other body parts during larval systemic growth. Subsequent histolysis occurs after growth arrest during metamorphosis (Berry and Baehrecke, 2007; Thummel, 2002; Xu et al., 2020).

The well-documented functions of *Drosophila* salivary glands are to produce glue proteins that contribute to the attachment of the pupa to a solid surface prior to metamorphosis (Duan et al., 2020; Fraenkel, 1952; Fraenkel and Brookes, 1953). Salivary glands also secrete glycosylated mucin or nondigestive enzymes that aid in the lubrication of food during the larval period (Costantino et al., 2008; Farkas et al., 2014; Riddiford, 1993; Syed et al., 2008). These products are secreted into the lumen of salivary glands via an exocrine way and released through the connected duct. Interestingly, previous studies in mammals have reported that salivary glands may have endocrine roles as well. A parotin hormone has been suggested to be produced from bovine salivary glands and probably secreted into the general circulation (Aonuma et al., 1980; Ishizaka and Tsujii, 1994; Ito, 1960). In addition, a humoral factor, possibly epidermal growth factor, may be released from mouse/rat salivary glands to stimulate cell proliferation in the regenerating liver (Cohen, 1962; Jones et al., 1995; Noguchi et al., 1991). Despite these anecdotal reports, the role of salivary glands as an endocrine organ in animals, including insects, has not been rigorously established.

Animal systemic growth is regulated mainly by two classic nutrient-sensing pathways, insulin/insulin-like growth factor signaling (IIS) and mechanistic target of rapamycin (mTOR) signaling (Boulan et al., 2015). In *Drosophila*, insulin-like peptide 2 (Dilp2) is secreted from the insulin-producing cells (IPCs) located in the larval brain and functions as a master regulator of systemic growth (Boulan et al., 2015; Okamoto and Yamanaka, 2015; Texada et al., 2020; Wu and Brown, 2006). Genetically ablating the IPCs causes growth retardation (Rulifson

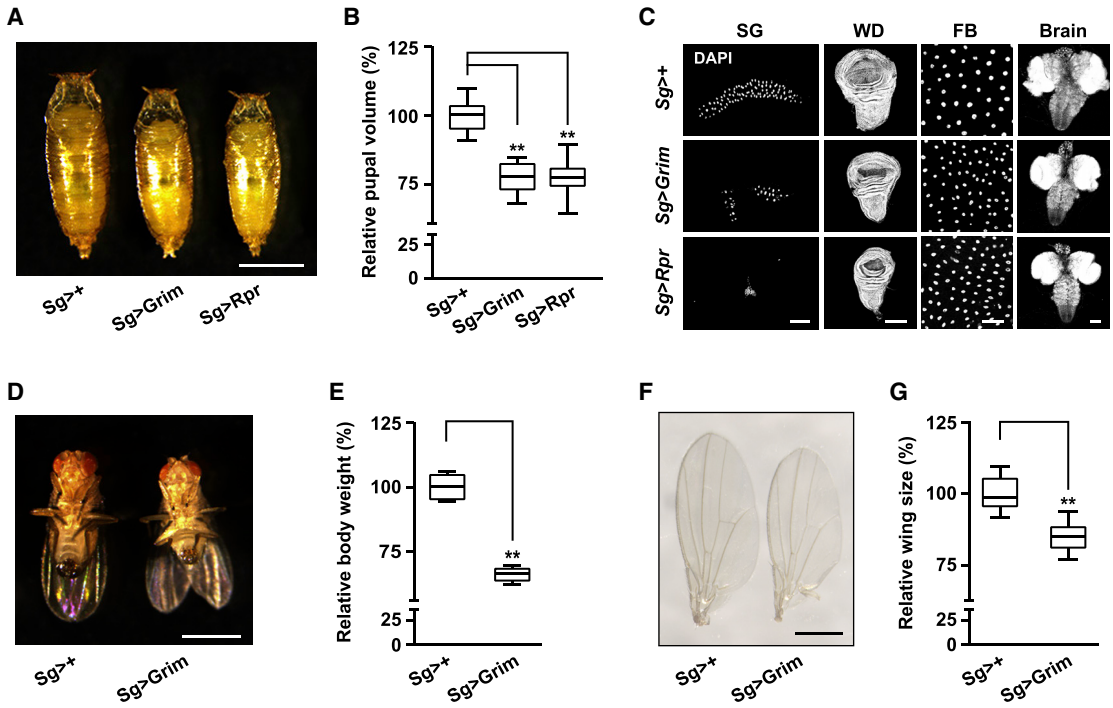


**Figure 1. Ablation of the salivary glands impairs systemic growth**

(A and B) Genetic ablation of *Drosophila* salivary glands decreases pupal volume. Scale bar, 1 mm.

(C) Salivary gland ablation impairs the size of larval organs at 120 h AEL. Salivary glands are almost undetectable after genetic ablation. Scale bar for salivary gland (SG) and wing disc (WD), 200 μm; Scale bar for fat body (FB) and brain, 100 μm; AEL, after egg laying.

(D–G) Effects of salivary gland ablation on adult body size (D), body weight (E), and wing size (F, G). Scale bar for body size, 1 mm; Scale bar for wing size, 0.5 mm. All experiments were conducted with three biological replicates. Data are presented as the mean ± SE (error bars). For the significance test: **p <0.01 versus the control. See also Figure S1.

et al., 2002), and *Dilp2* overexpression promotes growth (Ikeya et al., 2002). In addition, mTOR signaling in the fat body, a nutrient-sensing organ, regulates larval growth by coupling with IIS signaling (Colombani et al., 2003; Geminard et al., 2009; Koyama et al., 2013; Texada et al., 2020). Although salivary gland growth is synchronized with organism growth in *Drosophila*, whether it plays endocrine roles in systemic growth remains unclear.

Here, we identify in *Drosophila* a salivary gland-derived secreted factor (Sgsf) that is secreted into the hemolymph and that regulates systemic growth. We show that genetic ablation of *Drosophila* salivary glands decreases the size of both the body and organs. A liquid chromatography-tandem mass spectrometry (LC-MS/MS) analysis identifies that Sgsf is absent in the hemolymph after salivary gland ablation. Further, we confirm that larval salivary gland-specific Sgsf is secreted into the hemolymph and its secretion is undetectable following *Sgsf* knockout or signal peptide deletion. In addition, *Sgsf* knockout phenocopies the effects of salivary gland ablation and retards systemic growth by suppressing the secretion of Dilp2 in brain IPCs and mTOR signaling in the fat body. These findings demonstrate an endocrine role of salivary glands in the control of systemic growth and provide novel insights into inter-organ communication between the salivary gland and other body parts.

## RESULTS

### Ablation of the salivary glands retards systemic growth

To determine novel functions of the salivary glands, we genetically ablated them during the *Drosophila* larval stage via ectopic expression of the apoptosis-inducing genes *Grim* or *Rpr* using the *Sg-Gal4* driver, which is specifically expressed in salivary glands (Figure S1A). Strikingly, ablation of salivary glands decreased pupal volume as well as the size of larval wing disc, fat body cells, and brain at 120 h after egg laying (AEL) (Figures 1A–1C and S1B). The larval-pupal transition was also delayed following salivary gland ablation (Figure S1C). In addition, the ablation of salivary glands similarly decreased the body size, body weight, and wing size of adult flies (Figures 1D–1G). Collectively, our results indicate that *Drosophila* salivary gland ablation retards systemic growth.

Given that the food where *Drosophila* larvae with ablated salivary glands were raised was somewhat dry and hard, we next asked whether this food condition influences systemic growth. Interestingly, blue dye food experiments revealed that the salivary gland-ablated larvae could feed and digest food normally (Figure S1D). We further mixed an equal number of GFP-labeled wild type larvae with salivary gland-ablated larvae to keep the food wet and soft, and found that salivary gland-ablated larvae still developed into smaller pupae (Figure S1E). In addition,

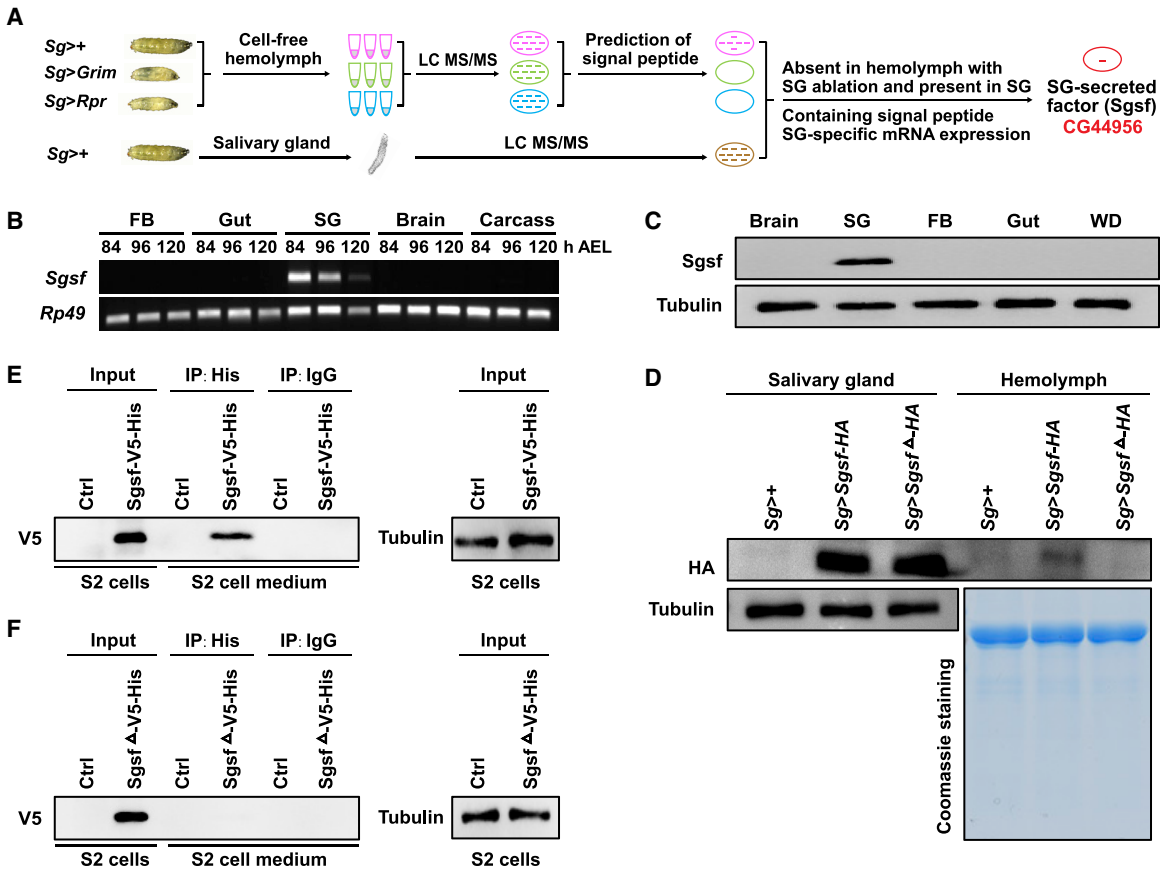


**Figure 2. Salivary gland-derived Sgsf peptide is secreted into the hemolymph**

(A) Schematic diagram for salivary gland ablation-based identification of Sgsf peptides. Cell-free hemolymph was isolated from *Drosophila* larvae at 120 h AEL. SG, Salivary gland.

(B and C) mRNA expression (B) and protein expression (C) of Sgsf in multiple tissues during the third larval instar were analyzed using semiquantitative RT-PCR and western blotting, respectively. FB, Fat body; SG, Salivary gland.

(D) *In vivo* examination of the secretion ability of Sgsf proteins in *Drosophila* larvae. HA-tagged Sgsf protein could be detected in the cell-free hemolymph following salivary gland-specific overexpression of the full-length form of Sgsf but not of a truncated form without signal peptide. Tubulin and Coomassie staining were used as the loading controls for salivary gland and hemolymph, respectively.

(E and F) Secretion of Sgsf proteins in *Drosophila* S2 cells. Immunoprecipitation (IP) was performed in cell-free medium from cultured *Drosophila* S2 cells overexpressing either *Sgsf*-V5-His or *Sgsf*$^{\Delta}$-V5-His using an anti-His antibody. Sgsf-V5-His (E), but not Sgsf$^{\Delta}$-V5-His without signal peptide (F), is secreted. AEL, after egg laying; Ctrl, Control. See also Figure S2.

because glue and mucin proteins are the main products of *Drosophila* salivary glands and may contribute to food lubrication (Abrams et al., 2003; Beckendorf and Kafatos, 1976; Kaieda et al., 2017; Kramerov et al., 1997; Syed et al., 2008), we performed salivary gland-specific knockdown of several *Mucin* and *Glue* genes, but observed no change in pupal volume (Figure S1F). Collectively, the food condition caused by salivary gland ablation had no obvious impact on systemic growth.

## Salivary gland-derived Sgsf peptide is secreted into the hemolymph

Increasing evidence in *Drosophila* reveals that several nonneuronal tissues, such as the fat body and wing discs, can secrete peptides via endocrine signaling into the hemolymph to regulate body growth and development (Agrawal et al., 2016; Boulan et al., 2015; Colombani et al., 2012; Delanoue et al., 2016; Garelli et al., 2012; Rajan and Perrimon, 2012; Texada et al., 2020). As salivary gland ablation induced retardation of systemic growth, it raised the possibility that salivary glands might secrete a growth factor-like peptide into the hemolymph to regulate systemic growth in an endocrine manner. To identify potential salivary gland-derived peptides that are present in the proteome of normal salivary glands (especially showing salivary gland-specific expression), absent in the proteome of cell-free hemolymph following salivary gland ablation, and have a signal peptide, we performed LC-MS/MS analysis to investigate the changes in the proteome of cell-free hemolymph at 120 h AEL following salivary gland ablation (Figure 2A). This analysis identified 544 proteins in the hemolymph of the control, 294 proteins in *Sg* > *Grim* hemolymph, and 191 proteins in *Sg* > *Rpr* hemolymph (Table S1). Comparatively, 266 proteins from the cell-free hemolymph of the control were absent in the cell-free hemolymph of larvae with

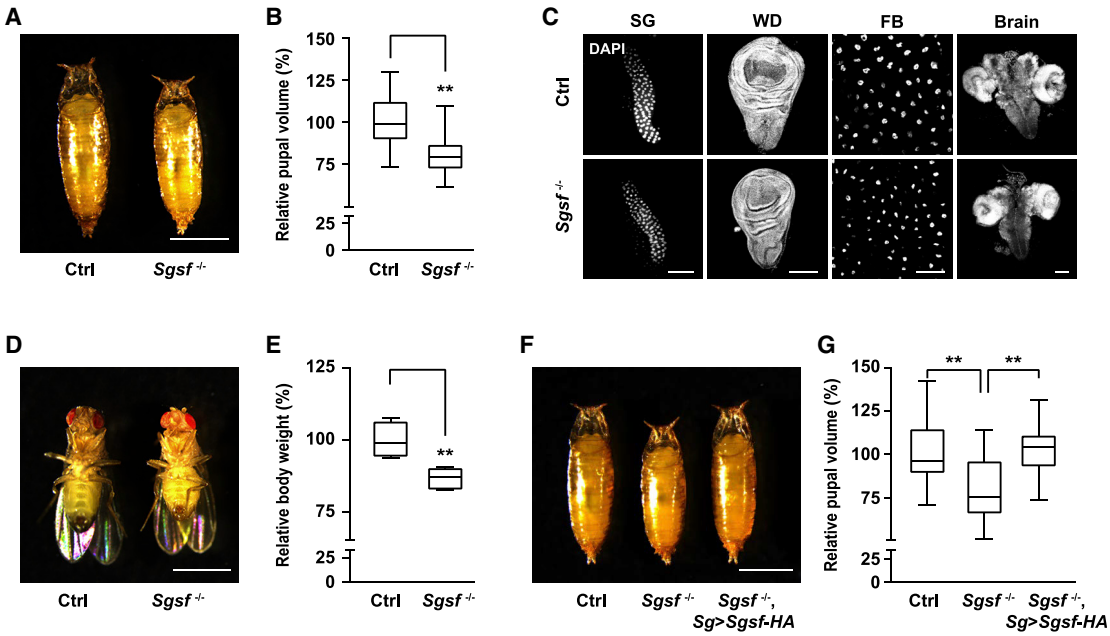


**Figure 3. CRISPR/Cas9-mediated *Sgsf* knockout suppresses systemic growth**

(A-E) CRISPR/Cas9-mediated *Sgsf* knockout affects pupal volume (A-B), larval organ size (C), adult body size (D), and adult body weight (E). The organ size was measured at 120 h AEL. Scale bars for pupal volume and adult body size, 1 mm. Scale bar for salivary gland (SG) and wing disc (WD), 200 μm; Scale bar for fat body (FB) and brain, 100 μm.

(F-G) Enhanced *Sgsf* expression in salivary glands rescues the decreased pupal volume caused by *Sgsf* knockout. Scale bar, 1 mm. Wild type stock Canton-S is used as the control (Ctrl). All experiments were conducted with three biological replicates. Data are presented as the mean ± SE (error bars). For the significance test: **p <0.01 versus the control. See also Figure S3.

salivary gland ablation (Table S1). Further comparative proteomic analysis revealed that 158 of the 266 proteins were present in the normal salivary gland proteome (Table S1). In silico analysis predicted that 15 of the 158 proteins had signal peptide sequences (Table S1). Next, a semiquantitative RT-PCR analysis showed that among the 15 proteins, a previously uncharacterized gene CG44956, which encodes a protein composing of 162 amino acid residues, was specifically expressed in larval salivary glands (Figures 2B and S2A), which was consistent with its protein expression (Figures 2C and S2B). Notably, this putative salivary gland-derived secreted factor (Sgsf) from *Drosophila melanogaster* has orthologs in other *Drosophila* species (Figure S2C).

We next examined the secretion activity of Sgsf protein. First, we analyzed the dynamic changes in Sgsf protein levels in salivary glands and cell-free hemolymph during the third larval (L3) stage from 84 to 120 h AEL. In contrast to a gradual accumulation in salivary glands, Sgsf protein levels gradually decreased in cell-free hemolymph (Figures S2D–S2F). These dynamic changes indicated that Sgsf proteins from salivary glands may be secreted into the hemolymph and that this secretion is decreased at the end of the L3 stage. Second, a previous study in *Drosophila* salivary glands has reported that the glue protein Sgs3 is secreted from cells into the lumen at the end of the L3 stage (Kaieda et al., 2017). Based on the Sgs3-GFP reporter, we observed that Sgs3 was secreted into the lumen of salivary glands at the end of the L3 stage, but Sgsf did not colocalize with Sgs3, indicating that Sgsf is not secreted into the lumen (Figure S2G and Video S1). Third, we investigated the secretion ability of Sgsf in both transgenic flies and transfected *Drosophila* S2 cells. Sgsf protein containing a signal peptide could be detected either in the hemolymph of the larvae overexpressing *Sgsf* in salivary glands or in the cultured medium of S2 cells following transient overexpression (Figures 2D, 2E, and S2H). However, overexpression of a truncated form of Sgsf lacking the signal peptide was undetectable (Figures 2D and 2F, and S2H). Altogether, these results demonstrate that *Drosophila* Sgsf is secreted from salivary glands into the hemolymph.

## Sgsf promotes systemic growth

To characterize the role of *Drosophila* Sgsf in systemic growth during the larval period, we performed site-specific knockout of the *Sgsf* gene using the CRISPR/Cas9 system. A *Sgsf* mutant allele with two genomic deletions induced by different sgRNAs was generated (Figure S3A), and Sgsf proteins could not be detected in either salivary glands or the hemolymph of *Sgsf* $^{-/-}$ animals (Figure S3B). Compared to controls, *Sgsf* $^{-/-}$ animals phenocopied salivary gland ablation and exhibited a decrease in pupal volume, the size of larval organs, the nuclear size of salivary gland and fat body cells, and the size and weight of the adult body (Figures 3A–3E and S3C). However, *Sgsf* knockout did not affect developmental timing (Figure S3D). Moreover, we generated two RNAi lines targeting different regions of the *Sgsf* gene and observed that SG-specific *Sgsf* RNAi decreased pupal volume (Figures S3E–S3G). Conversely, SG-specific *Sgsf* overexpression increased pupal volume and the size of larval organs

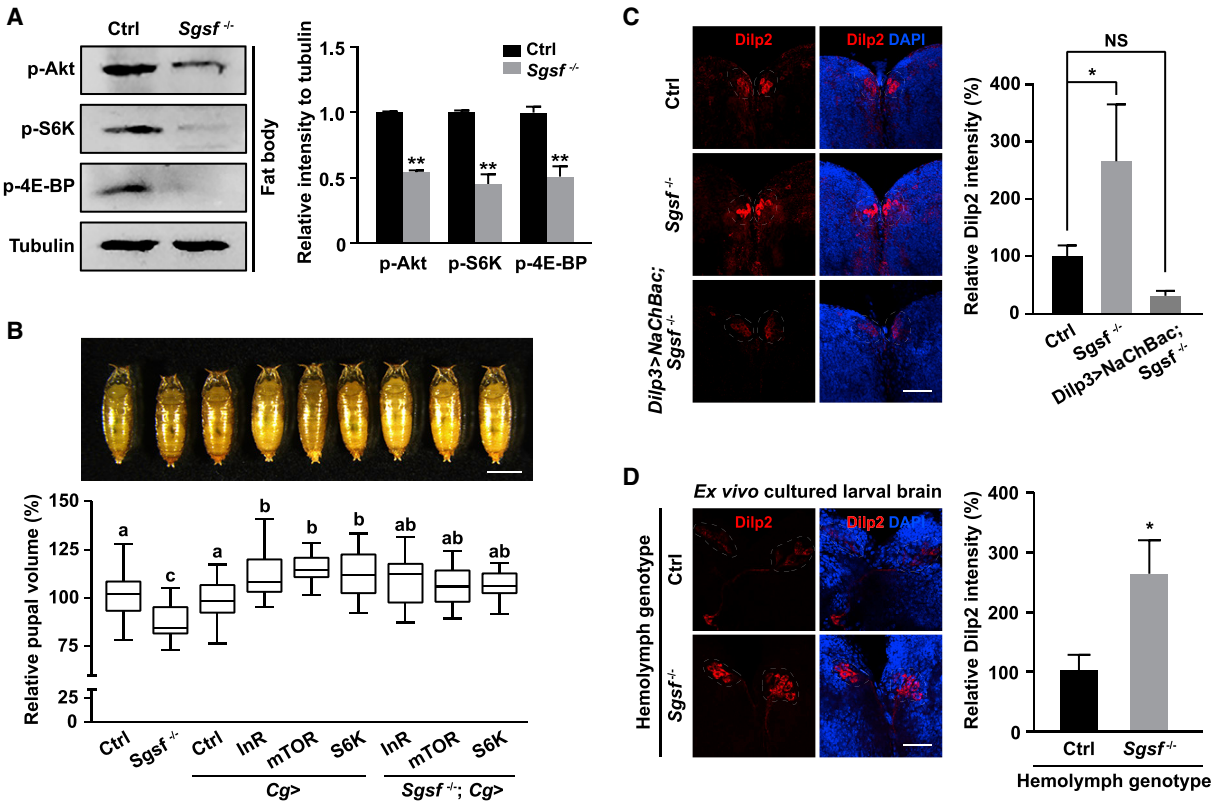


**Figure 4. Sgsf regulates systemic growth by modulating IIS/mTOR signaling in the fat body and Dilp2 secretion from the IPCs**

(A) Effects of *Sgsf* knockout on IIS/mTOR signaling in fat body at 120 h AEL. The protein levels were normalized to that of tubulin protein.

(B) The pupal volume reduction associated with *Sgsf* knockout can be rescued by enhancing IIS/mTOR signaling in the fat body. Scale bar, 1 mm.

(C) *Sgsf* knockout causes Dilp2 accumulation in the IPCs at 120 h AEL, and enhanced expression of *NaChBac* in the IPCs rescues Dilp2 secretion. Scale bar, 50 μm.

(D) *Sgsf* $^{-/-}$ animal hemolymph decreased Dilp2 secretion from *ex vivo* cultured brains of *Drosophila* larvae at 120 h AEL. Wild type stock Canton-S is used as the control. All experiments were conducted with three biological replicates. Data are presented as the mean ± SE (error bars). For the significance test: *p <0.05 and **p <0.01 versus the control. Different letters above bars denote significant differences ($P < 0.05$). NS means no significant difference. AEL, after egg laying; Ctrl, Control. See also Figures S3 and S4.

(Figures S3H and S3I). The decrease in pupal volume caused by *Sgsf* knockout could also be rescued by SG-specific *Sgsf* overexpression (Figures 3F and 3G). Altogether, these data suggest that salivary gland-derived Sgsf is secreted into the hemolymph to promote systemic growth.

## Sgsf regulates systemic growth by modulating Dilp2 secretion from the IPCs and IIS/mTOR signaling in the fat body

The IIS/mTOR signaling pathway is the main regulator of insect systemic growth (Boulan et al., 2015; Texada et al., 2020). Thus, we tested whether Sgsf modulates IIS/mTOR signaling. Interestingly, phosphorylation levels of Akt, S6K, and 4E-BP, key effectors of IIS/mTOR signaling, were decreased in the fat body of *Sgsf* $^{-/-}$ animals (Figure 4A). Consistently, the levels of phosphorylated Akt, S6K, and 4E-BP were also decreased in the fat body following salivary gland ablation (Figure S4A). Furthermore, increasing IIS/mTOR signaling in the fat body of *Sgsf* $^{-/-}$ animals by using *Cg-Gal4* to drive an overexpression of *mTOR*, *S6K*, or insulin receptor *InR* rescued the decreased pupal volume of *Sgsf* mutant animals (Figure 4B). Finally, feeding salivary gland-ablated larvae with high-protein food could also rescue the abnormal size associated with salivary gland ablation (Figure S4B).

Given that insulin-like peptide Dilp2 secreted from the IPCs of the brain plays key role in regulating systemic growth (Brogiolo et al., 2001; Rulifson et al., 2002), we next investigated Sgsf regulation of Dilp2 action. First, we examined the effects of Sgsf expression changes on the level of Dilp2 in the IPCs and hemolymph. Compared to the wild type at 120 h AEL, *Sgsf* knockout caused Dilp2 accumulation in the IPCs (Figure 4C) but a decrease in Dilp2 levels in the hemolymph of *Sgsf* $^{-/-}$ larvae (Figure S4C). We further noted that *Sgsf* knockout weakly decreased *Dilp2* mRNA expression in the brain-ring gland complex and had no effect on the mRNA expression of *Dilp3* and *Dilp5* at 120 h AEL (Figure S4D), indicating that the *Sgsf* knockout-induced Dilp2 accumulation in the IPCs is not related to the change in *Dilp2* mRNA levels. Notably, either salivary gland ablation or SG-specific *Sgsf* knockdown also led to Dilp2 accumulation in the IPCs (Figures S4E and S4F), but SG-specific *Sgsf*

overexpression promoted Dilp2 secretion (Figure S4G). Second, secreted Upd2 from the fat body has been shown to promote Dilp2 secretion (Boulan et al., 2015; Rajan and Perrimon, 2012), and Impl2 secreted from multiple tissues plays an antagonistic function against Dilp2 (Kwon et al., 2015; Lee et al., 2018). However, we did not observe a change in *Upd2* expression in the fat body or *Impl2* expression in multiple tissues of *Sgsf* $^{-/-}$ animals at 120 h AEL (Figures S4H and S4I). Third, as overexpression of the *bacterial sodium channel* (*NaChBac*) in the IPCs can promote Dilp2 secretion (Rajan and Perrimon, 2012), we tested whether overexpression of *NaChBac* in the IPCs could rescue the phenotype associated with loss of *Sgsf*. Strikingly, both Dilp2 accumulation and reduced pupal volume could be restored by *Dilp3-Gal4* driver-mediated *NaChBac* overexpression in the IPCs of the *Sgsf* $^{-/-}$ larvae (Figures 4C and S4J). Finally, we performed an *ex vivo* assay to examine the effect of Sgsf on Dilp2 secretion from the IPCs. We incubated *ex vivo* cultured brains from *Drosophila* larvae at 120 h AEL with the hemolymph from the wild type and *Sgsf* $^{-/-}$ animals, respectively. Subsequent immunostaining revealed that compared with the control, *Sgsf* $^{-/-}$ animal hemolymph decreased Dilp2 secretion from the IPCs (Figure 4D). Similarly, recombinant Sgsf proteins could promote Dilp2 secretion from the IPCs in *ex vivo* cultured brains (Figure S4K). Taken together, our results indicate that Sgsf regulates systemic growth by promoting the release of Dilp2 from the IPCs and modulating IIS/mTOR signaling in the fat body.

## DISCUSSION

The insect salivary gland is a classic example of an exocrine gland that synthesizes products secreted into the lumen (Riddiford, 1993), being important for the attachment of the pupa to a surface and for lubricating food (Costantino et al., 2008; Duan et al., 2020; Farkas et al., 2014; Riddiford, 1993; Syed et al., 2008). Our study in *Drosophila* identifies a salivary gland-derived peptide, Sgsf, as an endocrine factor secreted into the hemolymph that systemically regulates larval growth via IIS/mTOR signaling.

Glands are typically classified based on their abilities to synthesize substances for release into the general circulation via endocrine mechanism as well as into cavities inside the body or its outer surface via exocrine mechanism. Some glands such as the mammalian pancreas and kidney have both endocrine and exocrine functions (Bailie, 1992; Henderson et al., 1981; Leung, 2010; Mastracci and Sussel, 2012). Previous studies in mice and rats have proposed that epidermal growth factor may be released from salivary glands to mediate the proliferative response in the regenerating liver (Cohen, 1962; Jones et al., 1995; Noguchi et al., 1991). Our findings in *Drosophila* provide the first evidence, to our knowledge, that salivary glands have endocrine functions in promoting larval systemic growth, establishing a novel crosstalk between salivary glands and other organs.

Insect systemic growth is mainly regulated by insulin-like peptide-mediated IIS/mTOR signaling (Boulan et al., 2015; Kannan and Fridell, 2013; Okamoto and Yamanaka, 2015; Texada et al., 2020). Dilp2 secreted from brain IPCs functions as a core regulator to promote insect systemic growth (Ikeya et al., 2002; Rulifson et al., 2002). Recent reports have shown that several circulating factors are involved in Dilp2 secretion during the larval period, including short neuropeptide F from glucose-sensing CN neurons in the brain (Oh et al., 2019), and Eiger, Stunted, Upd2, growth-blocking peptide, and CCHamide-2 from the fat body (Agrawal et al., 2016; Andersen et al., 2015; Delanoue et al., 2016; Koyama and Mirth, 2016; Rajan and Perrimon, 2012; Sano et al., 2015). Our present data demonstrate that Sgsf peptides secreted from larval salivary glands contribute to promote Dilp2 secretion, revealing the coupling of the salivary gland with brain IPCs in regulating systemic growth.

Previous reports have shown that another insulin-like peptide Dilp8 and retinoids from damaged imaginal discs reduce the larval growth rate and delays the onset of metamorphosis (Colombani et al., 2012; Garelli et al., 2012; Halme et al., 2010). This is similar to our observation that salivary gland ablation delays metamorphosis, but different from the finding that *Sgsf* knockout does not affect developmental timing. Whether Sgsf communicates with Dilp8 or that salivary glands secrete other factors in addition to Sgsf to regulate developmental timing remains to be investigated.

The timing of Sgsf expression in early third instar of *Drosophila* larvae is intriguing because *Drosophila* larvae pass the critical weight (CW) checkpoint approximately 12 h after the second larval molt, an irreversible decision at the early L3 stage for ensuring that larvae have acquired sufficient nutrients to develop into adults (Edgar, 2006; Zeng et al., 2020). A low-level ecdysone pulse appears around the CW checkpoint and activates the expression of target genes, such as glue protein genes (Andres et al., 1993; Kaieda et al., 2017; Texada et al., 2020). The increasing expression of *Drosophila Sgsf* after the CW checkpoint raises the possibility that Sgsf may be transcriptionally regulated by ecdysone. Our preliminary investigation revealed that SG-specific knockdown of the ecdysone receptor gene *EcR* at the early L3 stage decreased pupal volume and downregulated *Sgsf* transcription (Figures S4L and S4M), suggesting that Sgsf expression in salivary glands may be activated by ecdysone at the early L3 stage. Moreover, given that at the end of larval development, Sgsf secretion is decreased (Figure S2F), and high ecdysone peak causes the cessation of larval growth (Rewitz et al., 2013; Texada et al., 2020), we further analyzed whether ecdysone peak at the late L3 stage is involved in regulating Sgsf secretion. The result showed that *EcR* knockdown in the salivary glands at the late L3 stage increased Sgsf protein level in the hemolymph (Figure S4N), indicating that ecdysone represses Sgsf secretion at the end of the larval period. Taken together, our data should help further investigation of ecdysone regulation of Sgsf action in larval systemic growth.

### Limitations of the study

Our study demonstrates in *Drosophila* that salivary gland-derived Sgsf peptide is secreted into the hemolymph to regulate systemic growth via IIS/mTOR signaling. However, the observation that *Sgsf* knockout has no effect on developmental timing is different from the finding that salivary gland ablation delays larval-pupal transition, indicating the possibility that salivary gland may secrete other factors in addition to Sgsf to regulate developmental timing. In addition, characterization of the Sgsf receptor will be required to decipher the mechanism by which Sgsf secreted from salivary glands acts on the brain to promote Dilp2 secretion.

## STAR★METHODS

Detailed methods are provided in the online version of this paper and include the following:

- KEY RESOURCES TABLE
- RESOURCE AVAILABILITY
  - Lead contact
  - Materials availability
  - Data and code availability
- EXPERIMENTAL MODEL AND SUBJECT DETAILS
  - *Drosophila* stocks and cultivation
- METHOD DETAILS
  - Generation of mutant and transgenic flies
  - Size and weight measurement
  - Hemolymph sample preparation and LC-MS/MS analysis
  - Developmental timing
  - Measurement of feeding and digestion abilities
  - Semiquantitative RT-PCR and quantitative RT-PCR (RT-qPCR)
  - Western blotting
  - Immunostaining
  - Immunoprecipitation
  - *Ex vivo* brain culture
- QUANTIFICATION AND STATISTICAL ANALYSIS

## SUPPLEMENTAL INFORMATION

Supplemental information can be found online at https://doi.org/10.1016/j.celrep.2022.110397.

## ACKNOWLEDGMENTS

We thank Drs. Jianquan Ni and Luping Liu at TsingHua Fly Center and Wei Wu at CAS Center for Excellence in Molecular Cell Science for their technical support in the generation of both transgenic lines and CRISPR/Cas9-based mutants. We thank Dr. Lei Xue at Tongji University for fly lines. This work was funded by the National Natural Science Foundation of China (31772679, 31572464, and 32070496), the Natural Science Foundation of Chongqing (cstc2020jcyj-cxttX0001 and cstc2019jcyj-msxmX0446), the Municipal Graduate Student Research Innovation Project of Chongqing (CYB19114), and the Fundamental Research Funds for the Central Universities (XDJK2019D007). N.P. is an HHMI investigator.

## AUTHOR CONTRIBUTIONS

D.C., Q.X., and N.P. conceived and designed the project. Z.L., W.Q., W.S., T.Z., Y.Y., W.W., L.W., D.Z., and Y.L. performed the experiments. Z.L., W.Q., D.C., Q.X., and N.P. analyzed the data. D.C., Z.L., and W.Q. drafted the paper. Q.X. and N.P. edited the paper.

## DECLARATION OF INTERESTS

The authors declare no competing interests.

Received: June 2, 2021
Revised: November 10, 2021
Accepted: January 26, 2022
Published: February 15, 2022

## REFERENCES

Abrams, E.W., Vining, M.S., and Andrew, D.J. (2003). Constructing an organ: the *Drosophila* salivary gland as a model for tube formation. Trends Cell Biol. *13*, 247–254.

Agrawal, N., Delanoue, R., Mauri, A., Basco, D., Pasco, M., Thorens, B., and Leopold, P. (2016). The *Drosophila* TNF Eiger is an adipokine that acts on insulin-producing cells to mediate nutrient response. Cell Metab. *23*, 675–684.

Andersen, D.S., Colombani, J., Palmerini, V., Chakrabandhu, K., Boone, E., Rothlisberger, M., Toggweiler, J., Basler, K., Mapelli, M., Hueber, A.O., et al. (2015). The *Drosophila* TNF receptor grindelwald couples loss of cell polarity and neoplastic growth. Nature *522*, 482–486.

Andres, A.J., Fletcher, J.C., Karim, F.D., and Thummel, C.S. (1993). Molecular analysis of the initiation of insect metamorphosis: a comparative study of *Drosophila* ecdysteroid-regulated transcription. Dev. Biol. *160*, 388–404.

Aonuma, S., Kohama, Y., Komiyama, Y., Fujimoto, S., and Nomura, M. (1980). Amino acid sequence of an active fragment, Fr. AA-1, of salivary gland hormone. Chem. Pharm. Bull. (Tokyo) *28*, 417–423.

Bailie, M.D. (1992). Development of the endocrine function of the kidney. Clin. Perinatol *19*, 59–68.

Beckendorf, S.K., and Kafatos, F.C. (1976). Differentiation in the salivary glands of *Drosophila melanogaster*: characterization of the glue proteins and their developmental appearance. Cell *9*, 365–373.

Berry, D.L., and Baehrecke, E.H. (2007). Growth arrest and autophagy are required for salivary gland cell degradation in *Drosophila*. Cell *131*, 1137–1148.

Boulan, L., Milan, M., and Leopold, P. (2015). The systemic control of growth. Cold Spring Harb Perspect. Biol. *7*, a019117.

Bradley, P.L., Haberman, A.S., and Andrew, D.J. (2001). Organ formation in *Drosophila*: specification and morphogenesis of the salivary gland. Bioessays *23*, 901–911.

Brogiolo, W., Stocker, H., Ikeya, T., Rintelen, F., Fernandez, R., and Hafen, E. (2001). An evolutionarily conserved function of the *Drosophila* insulin receptor and insulin-like peptides in growth control. Curr. Biol. *11*, 213–221.

Camelo, C., and Luschnig, S. (2021). Cells into tubes: Molecular and physical principles underlying lumen formation in tubular organs. Curr. Top Dev. Biol. *143*, 37–74.

Cohen, S. (1962). Isolation of a mouse submaxillary gland protein accelerating incisor eruption and eyelid opening in the new-born animal. J. Biol. Chem. *237*, 1555–1562.

Colombani, J., Andersen, D.S., and Leopold, P. (2012). Secreted peptide Dilp8 coordinates *Drosophila* tissue growth with developmental timing. Science *336*, 582–585.

Colombani, J., Raisin, S., Pantalacci, S., Radimerski, T., Montagne, J., and Leopold, P. (2003). A nutrient sensor mechanism controls *Drosophila* growth. Cell *114*, 739–749.

Costantino, B.F., Bricker, D.K., Alexandre, K., Shen, K., Merriam, J.R., Antoniewski, C., Callender, J.L., Henrich, V.C., Presente, A., and Andres, A.J. (2008). A novel ecdysone receptor mediates steroid-regulated developmental events during the mid-third instar of *Drosophila*. PLoS Genet. *4*, e1000102.

Delanoue, R., Meschi, E., Agrawal, N., Mauri, A., Tsatskis, Y., McNeill, H., and Leopold, P. (2016). *Drosophila* insulin release is triggered by adipose Stunted ligand to brain Methuselah receptor. Science *353*, 1553–1556.

Duan, J., Zhao, Y., Li, H., Habernig, L., Gordon, M.D., Miao, X., Engstrom, Y., and Buttner, S. (2020). Bab2 functions as an ecdysone-responsive transcriptional repressor during *Drosophila* development. Cell Rep. *32*, 107972.

Edgar, B.A. (2006). How flies get their size: genetics meets physiology. Nat. Rev. Genet. *7*, 907–916.

Edgar, B.A., Zielke, N., and Gutierrez, C. (2014). Endocycles: a recurrent evolutionary innovation for post-mitotic cell growth. Nat. Rev. Mol. Cell Biol *15*, 197–210.

Farkas, R., Datkova, Z., Mentelova, L., Low, P., Benova-Liszekova, D., Beno, M., Sass, M., Rehulka, P., Rehulkova, H., Raska, O., et al. (2014). Apocrine

secretion in *Drosophila* salivary glands: subcellular origin, dynamics, and identification of secretory proteins. PLoS One *9*, e94383.

Fraenkel, G. (1952). A function of the salivary glands of the larvae of *Drosophila* and other flies. Biol. Bull. *103*, 285–286.

Fraenkel, G., and Brookes, V.J. (1953). The process by which the puparia of many species of flies become fixed to a substrate. Biol. Bull. *105*, 442–449.

Garelli, A., Gontijo, A.M., Miguela, V., Caparros, E., and Dominguez, M. (2012). Imaginal discs secrete insulin-like peptide 8 to mediate plasticity of growth and maturation. Science *336*, 579–582.

Geminard, C., Rulifson, E.J., and Leopold, P. (2009). Remote control of insulin secretion by fat cells in *Drosophila*. Cell Metab *10*, 199–207.

Halme, A., Cheng, M., and Hariharan, I.K. (2010). Retinoids regulate a developmental checkpoint for tissue regeneration in Drosophila. Curr. Biol. *20*, 458–463.

Henderson, J.R., Daniel, P.M., and Fraser, P.A. (1981). The pancreas as a single organ: the influence of the endocrine upon the exocrine part of the gland. Gut *22*, 158–167.

Ikeya, T., Galic, M., Belawat, P., Nairz, K., and Hafen, E. (2002). Nutrient-dependent expression of insulin-like peptides from neuroendocrine cells in the CNS contributes to growth regulation in *Drosophila*. Curr. Biol. *12*, 1293–1300.

Ishizaka, S., and Tsujii, T. (1994). Parotin subunit and its synthetic peptide possess interleukin 1-like activity and exert stimulating effects on liver cells and brain cells. Cytokine *6*, 265–271.

Ito, Y. (1960). Parotin: a salivary gland hormone. Ann. N. Y Acad. Sci. *85*, 228–312.

Jones, D.E., Jr., Tran-Patterson, R., Cui, D.M., Davin, D., Estell, K.P., and Miller, D.M. (1995). Epidermal growth factor secreted from the salivary gland is necessary for liver regeneration. Am. J. Physiol. *268*, G872–G878.

Kaieda, Y., Masuda, R., Nishida, R., Shimell, M., O'Connor, M.B., and Ono, H. (2017). Glue protein production can be triggered by steroid hormone signaling independent of the developmental program in *Drosophila melanogaster*. Dev. Biol. *430*, 166–176.

Kannan, K., and Fridell, Y.W. (2013). Functional implications of *Drosophila* insulin-like peptides in metabolism, aging, and dietary restriction. Front. Physiol. *4*, 288.

Kondo, S., and Ueda, R. (2013). Highly improved gene targeting by germline-specific Cas9 expression in *Drosophila*. Genetics *195*, 715–721.

Koyama, T., Mendes, C.C., and Mirth, C.K. (2013). Mechanisms regulating nutrition-dependent developmental plasticity through organ-specific effects in insects. Front. Physiol. *4*, 263.

Koyama, T., and Mirth, C.K. (2016). Growth-blocking peptides as nutrition-sensitive signals for insulin secretion and body size regulation. PLoS Biol. *14*, e1002392.

Kramerov, A.A., Mikhaleva, E.A., Pochechueva, T.V., Rozovskii Ia, M., Baikova, N.A., and Gvozdev, V.A. (1997). The tissue localization and secretion of mucin-D in *Drosophila melanogaster*. Ontogenez *28*, 279–287.

Kwon, Y., Song, W., Droujinine, I.A., Hu, Y., Asara, J.M., and Perrimon, N. (2015). Systemic organ wasting induced by localized expression of the secreted insulin/IGF antagonist ImpL2. Dev. Cell *33*, 36–46.

Lee, G.J., Han, G., Yun, H.M., Lim, J.J., Noh, S., Lee, J., and Hyun, S. (2018). Steroid signaling mediates nutritional regulation of juvenile body growth via IGF-binding protein in *Drosophila*. Proc. Natl. Acad. Sci. U S A. *115*, 5992–5997.

Leung, P.S. (2010). Physiology of the pancreas. Adv. Exp. Med. Biol. *690*, 13–27.

Liu, Y., Mattila, J., Ventela, S., Yadav, L., Zhang, W., Lamichane, N., Sundstrom, J., Kauko, O., Grenman, R., Varjosalo, M., et al. (2017). PWP1 mediates nutrient-dependent growth control through nucleolar regulation of ribosomal gene expression. Dev. Cell *43*, 240–252.

Machado, D.R., Afonso, D.J., Kenny, A.R., Oztu Rk-Colak, A., Moscato, E.H., Mainwaring, B., Kayser, M., and Koh, K. (2017). Identification of octopaminergic neurons that modulate sleep suppression by male sex drive. Elife *6*, e23130.

Mastracci, T.L., and Sussel, L. (2012). The endocrine pancreas: insights into development, differentiation, and diabetes. Wiley Interdiscip. Rev. Dev. Biol. *1*, 609–628.

Meschi, E., Leopold, P., and Delanoue, R. (2019). An EGF-responsive neural circuit couples insulin secretion with nutrition in *Drosophila*. Dev. Cell *48*, 76–86.

Ni, J.Q., Liu, L.P., Binari, R., Hardy, R., Shim, H.S., Cavallaro, A., Booker, M., Pfeiffer, B.D., Markstein, M., Wang, H., et al. (2009). A *Drosophila* resource of transgenic RNAi lines for neurogenetics. Genetics *182*, 1089–1100.

Ni, J.Q., Markstein, M., Binari, R., Pfeiffer, B., Liu, L.P., Villalta, C., Booker, M., Perkins, L., and Perrimon, N. (2008). Vector and parameters for targeted transgenic RNA interference in *Drosophila melanogaster*. Nat. Methods *5*, 49–51.

Ni, J.Q., Zhou, R., Czech, B., Liu, L.P., Holderbaum, L., Yang-Zhou, D., Shim, H.S., Tao, R., Handler, D., Karpowicz, P., et al. (2011). A genome-scale shRNA resource for transgenic RNAi in *Drosophila*. Nat. Methods *8*, 405–407.

Noguchi, S., Ohba, Y., and Oka, T. (1991). Influence of epidermal growth factor on liver regeneration after partial hepatectomy in mice. J. Endocrinol. *128*, 425–431.

Oh, Y., Lai, J.S., Mills, H.J., Erdjument-Bromage, H., Giammarinaro, B., Saadipour, K., Wang, J.G., Abu, F., Neubert, T.A., and Suh, G.S.B. (2019). A glucose-sensing neuron pair regulates insulin and glucagon in *Drosophila*. Nature *574*, 559–564.

Okamoto, N., Viswanatha, R., Bittar, R., Li, Z., Haga-Yamanaka, S., Perrimon, N., and Yamanaka, N. (2018). A membrane transporter is required for steroid hormone uptake in *Drosophila*. Dev. Cell *47*, 294–305.

Okamoto, N., and Yamanaka, N. (2015). Nutrition-dependent control of insect development by insulin-like peptides. Curr. Opin. Insect Sci. *11*, 21–30.

Pirraglia, C., and Myat, M.M. (2010). Genetic regulation of salivary gland development in *Drosophila melanogaster*. Front. Oral Biol. *14*, 32–47.

Qian, W., Li, Z., Song, W., Zhao, T., Wang, W., Peng, J., Wei, L., Xia, Q., and Cheng, D. (2020). A novel transcriptional cascade is involved in Fzr-mediated endoreplication. Nucleic Acids Res. *48*, 4214–4229.

Rajan, A., and Perrimon, N. (2012). *Drosophila* cytokine unpaired 2 regulates physiological homeostasis by remotely controlling insulin secretion. Cell *151*, 123–137.

Redhai, S., Pilgrim, C., Gaspar, P., Giesen, L.V., Lopes, T., Riabinina, O., Grenier, T., Milona, A., Chanana, B., Swadling, J.B., et al. (2020). An intestinal zinc sensor regulates food intake and developmental growth. Nature *580*, 263–268.

Ren, X., Sun, J., Housden, B.E., Hu, Y., Roesel, C., Lin, S., Liu, L.P., Yang, Z., Mao, D., Sun, L., et al. (2013). Optimized gene editing technology for *Drosophila melanogaster* using germ line-specific Cas9. Proc. Natl. Acad. Sci. U S A. *110*, 19012–19017.

Rewitz, K.F., Yamanaka, N., and O'Connor, M.B. (2013). Developmental checkpoints and feedback circuits time insect maturation. Curr. Top Dev. Biol. *103*, 1–33.

Riddiford, L.M. (1993). In The Development of *Drosophila melanogaster*, M. Bate and A.M. Arias, eds. (Cold Spring Harbor Laboratory Press), pp. 899–939.

Rulifson, E.J., Kim, S.K., and Nusse, R. (2002). Ablation of insulin-producing neurons in flies: growth and diabetic phenotypes. Science *296*, 1118–1120.

Sano, H., Nakamura, A., Texada, M.J., Truman, J.W., Ishimoto, H., Kamikouchi, A., Nibu, Y., Kume, K., Ida, T., and Kojima, M. (2015). The nutrient-responsive hormone CCHamide-2 controls growth by regulating insulin-like peptides in the brain of *Drosophila melanogaster*. PLoS Genet. *11*, e1005209.

Song, W., Cheng, D., Hong, S., Sappe, B., Hu, Y., Wei, N., Zhu, C., O'Connor, M.B., Pissios, P., and Perrimon, N. (2017). Midgut-derived activin regulates glucagon-like action in the fat body and glycemic control. Cell Metab *25*, 386–399.

Syed, Z.A., Hard, T., Uv, A., and van Dijk-Hard, I.F. (2008). A potential role for *Drosophila* mucins in development and physiology. PLoS One *3*, e3041.

Texada, M.J., Koyama, T., and Rewitz, K. (2020). Regulation of body size and growth control. Genetics *216*, 269–313.

Thummel, C.S. (2002). Ecdysone-regulated puff genes 2000. Insect Biochem. Mol. Biol. *32*, 113–120.

Villoria, M.T., Ramos, F., Duenas, E., Faull, P., Cutillas, P.R., and Clemente-Blanco, A. (2017). Stabilization of the metaphase spindle by Cdc14 is required for recombinational DNA repair. EMBO J. *36*, 79–101.

Wang, T., Blumhagen, R., Lao, U., Kuo, Y., and Edgar, B.A. (2012). LST8 regulates cell growth via target-of-rapamycin complex 2 (TORC2). Mol. Cell Biol. *32*, 2203–2213.

Wu, Q., and Brown, M.R. (2006). Signaling and function of insulin-like peptides in insects. Annu. Rev. Entomol. *51*, 1–24.

Xu, T., Jiang, X., Denton, D., and Kumar, S. (2020). Ecdysone controlled cell and tissue deletion. Cell Death Differ. *27*, 1–14.

Yang, Y., Zhao, T., Li, Z., Qian, W., Peng, J., Wei, L., Yuan, D., Li, Y., Xia, Q., and Cheng, D. (2021). Histone H3K27 methylation-mediated repression of Hairy regulates insect developmental transition by modulating ecdysone biosynthesis. Proc. Natl. Acad. Sci. U S A. *118*, e2101442118.

Zeng, J., Huynh, N., Phelps, B., and King-Jones, K. (2020). Snail synchronizes endocycling in a TOR-dependent manner to coordinate entry and escape from endoreplication pausing during the Drosophila critical weight checkpoint. PLoS Biol. *18*, e3000609.

Zhai, Z., Boquete, J.P., and Lemaitre, B. (2018). Cell-specific Imd-NF-kappaB responses enable simultaneous antibacterial immunity and intestinal epithelial cell shedding upon bacterial infection. Immunity *48*, 897–910.

Zhang, T., Song, W., Li, Z., Qian, W., Wei, L., Yang, Y., Wang, W., Zhou, X., Meng, M., Peng, J., et al. (2018). Kruppel homolog 1 represses insect ecdysone biosynthesis by directly inhibiting the transcription of steroidogenic enzymes. Proc. Natl. Acad. Sci. U S A. *115*, 3960–3965.

Zielke, N., Edgar, B.A., and DePamphilis, M.L. (2013). Endoreplication. Cold Spring Harb Perspect. Biol. *5*, a012948.

## STAR★METHODS

### KEY RESOURCES TABLE

| REAGENT or RESOURCE | SOURCE | IDENTIFIER |
|---|---|---|
| Antibodies | | |
| Rabbit polyclonal anti-phospho-Akt | Cell Signaling | Cat# 4054; RRID: AB_331414 |
| Rabbit polyclonal anti-phospho-S6K | Cell Signaling | Cat# 9209; RRID: AB_2269804 |
| Rabbit polyclonal anti-phospho-4E-BP1 | Cell Signaling | Cat# 2855; RRID: AB_560835 |
| Rabbit monoclonal anti-HA tag | Cell Signaling | Cat# 5017; RRID: AB_10693385 |
| Mouse monoclonal anti-Tubulin | Beyotime | Cat# AT819 |
| HRP-conjugated goat anti-rabbit | Beyotime | Cat# A0208; RRID:AB_2892644 |
| HRP-conjugated goat anti-mouse | Beyotime | Cat# A0216; RRID:AB_2860575 |
| Rabbit polyclonal anti-Sgsf | This study | N/A |
| Rabbit polyclonal anti-Dilp2 | This study | N/A |
| Goat anti-rabbit Alexa Fluor 594 | Molecular Probes | Cat# A-11012; RRID: AB_141359 |
| Chemicals, peptides, and recombinant proteins | | |
| Protein Stabilizing Cocktail | Thermo Fisher | Cat# 89806 |
| NP-40 Lysis Buffer | Beyotime | Cat# P0013F |
| Alexa Fluor™ 488 Phalloidin | Invitrogen | Cat# A12379 |
| DAPI | Thermo Fisher | Cat# D1306 |
| Bromophenol Blue sodium salt | Sigma-Aldrich | Cat# B5525 |
| Sgsf recombinant proteins | This study | N/A |
| Critical commercial assays | | |
| NovoStart ® SYBR qPCR SuperMix Plus | Novoprotein | Cat# E096-01B |
| pEASY-Blunt Zero Cloning Kit | Transgen | Cat# CB501-02 |
| EasyScript One-Step gDNA Removal and cDNA Synthesis Super Mix | Transgen | Cat# AE311-03 |
| Deposited data | | |
| Proteomics data | This study | ProteomeXchange: PXD026372 |
| Experimental models: organisms/strains | | |
| *Sg-Gal4* | (Costantino et al., 2008) | N/A |
| *Dilp3-Gal4* | (Rajan and Perrimon, 2012) | N/A |
| *Cg-Gal4* | BDSC | #7011 |
| *Fkh-Gal4* | BDSC | #78060 |
| *UAS-Grim* | Gift from Dr. Lei Xue | N/A |
| *UAS-Rpr* | BDSC | #5824 |
| *UAS-InR* | BDSC | #8262 |
| *UAS-mTOR* | BDSC | #53727 |
| *UAS-S6K* | BDSC | #6912 |
| *UAS-NaChBac* | BDSC | #9466 |
| *Sgs3-GFP* | BDSC | #5885 |
| *UAS-Mucin4B* RNAi | BDSC | #67940 |
| *UAS-Sgs4* RNAi | BDSC | #63675 |
| *UAS-Sgs1* RNAi | TsingHua Fly Center | TH01653.N |
| *UAS-Sgs8* RNAi | TsingHua Fly Center | TH04781.N |
| *UAS-New glue1* RNAi | TsingHua Fly Center | TH03588.N |
| *UAS-Muc68ca* RNAi | TsingHua Fly Center | TH01755.N |
| *UAS-EcR* RNAi | TsingHua Fly Center | TH01841.N |
| *UAS-White* RNAi | TsingHua Fly Center | THU0558 |

(*Continued on next page*)

*Continued*

| REAGENT or RESOURCE | SOURCE | IDENTIFIER |
|---|---|---|
| *UAS-GFP* | TsingHua Fly Center | THJ0179 |
| *Tub-Gal80* $^{ts}$; TM2/TM6B | TsingHua Fly Center | THJ0187 |
| *Nos-Cas9* | TsingHua Fly Center | TH00787.N |
| Oligonucleotides | | |
| Primers are listed in Table S2 | This study | N/A |
| Software and algorithms | | |
| Fiji | Fiji | https://fiji.sc |
| Prism 5 | Graphpad | https://www.graphpad.com/scientific-software/prism/ |
| SPSS | IBM | https://www.ibm.com/products/spss-statistics |
| Zen | Carl Zeiss | N/A |

## RESOURCE AVAILABILITY

### Lead contact

Further information and requests for resources and reagents should be directed to and will be fulfilled by the lead contact, Daojun Cheng (chengdj@swu.edu.cn).

### Materials availability

All unique reagents or *Drosophila* lines generated in this study are available from the lead contact without restriction.

### Data and code availability

Proteomic data in this study have been deposited at ProteomeXchange via the PRIDE database and are publicly available as of the date of publication. Accession number is listed in the key resources table. This paper does not report original code. Any additional information required to reanalyze the data reported in this paper is available from the lead contact upon request.

## EXPERIMENTAL MODEL AND SUBJECT DETAILS

### *Drosophila* stocks and cultivation

*Drosophila* lines were reared at 25°C under a 12-h: 12-h light: dark cycle on standard food in a relative humidity of 70% unless noted otherwise (Qian et al., 2020; Zhang et al., 2018). For the analysis of larval organ size, pupal volume, adult weight, and wing size, male individuals were calculated. In addition, the second instar larvae regardless of gender were used to measure feeding and digestion abilities. Except for the above-mentioned experiments, all samples used in the present study were the third-instar larvae regardless of gender. The standard food used here contains the following contents in one liter of $H_2O$: 40 g sucrose, 42.4 g maltose, 5.5 g agar, 66.825 g yellow cornmeal, 9.2 g soy flour, 25 g dry yeast, 0.9 g p-hydroxybenzoic acid methyl ester (dissolved in 9 mL methanol), 1 g sodium benzoate, and 7 mL propionic acid. For high protein food, the standard food was supplemented with an additional 25 g dry yeast.

All *Drosophila* strains used in this study are shown in the key resources table. The following *Drosophila* stocks were used: *Sg-Gal4* was used to specifically drive gene expression in *Drosophila* salivary glands (Costantino et al., 2008). *Dilp3-Gal4* was used to specifically drive gene expression in *Drosophila* brain IPCs. Wild type (Canton-S) was used as the control. *UAS-Grim* was a gift from Professor Lei Xue at Tongji University. The following RNAi stocks were obtained from the Bloomington *Drosophila* Stock Center (BDSC): *UAS-Rpr* (#5824) (Zhai et al., 2018), *UAS-InR* (#8262) (Liu et al., 2017), *UAS-mTOR* (#53727) (Wang et al., 2012), *UAS-S6K* (#6912) (Redhai et al., 2020), *Cg-Gal4* (#7011) (Song et al., 2017), *UAS-NaChBac* (#9466) (Machado et al., 2017), *Sgs3-GFP* (#5885) (Okamoto et al., 2018), *UAS-Mucin4B* RNAi (#67940), *UAS-Sgs4* RNAi (#63675) and *Fkh*-Gal4 (#78060). *Drosophila* stocks from TsingHua Fly Center include: *UAS-Sgs1* RNAi (#TH01653.N), *UAS-Sgs8* RNAi (#TH04781.N), *UAS-New glue 1* RNAi (#TH03588.N), *UAS-Muc68ca* RNAi (#TH01755.N), *Nos-Cas9* (#TH00787.N), *UAS-EcR* RNAi (#TH01841.N), *UAS-white* RNAi (THU0558), *UAS-GFP* (THJ0179), and *Tub-Gal80*$^{ts}$; TM2/TM6B (THJ0187).

To conduct *EcR* knockdown in the salivary glands at different stages, the *UAS-EcR* RNAi line was crossed with the temperature-sensitive *Tub-Gal80*$^{ts}$; *Fkh-Gal4* line. For the analysis at the early L3 stage, the progenies were raised at 18°C for 3 days after hatching and then shifted to 29°C for 12 h. For the examination at the end of the larval period, the progenies were raised at 18°C for 5 days after hatching and then shifted to 29°C for 12 h.

## METHOD DETAILS

### Generation of mutant and transgenic flies

Two sgRNAs against the *Drosophila Sgsf* gene with single exon were designed as shown in Figure S3A using the online program (http://www.flyrnai.org/crispr/) and cloned into the U6b-sgRNA-short vector as previously described (Ren et al., 2013). Recombinant plasmids were co-microinjected into *Drosophila* embryos, and flies positive for *Sgsf* sgRNAs were identified. Subsequently, after crossing the *Nos-Cas9* line with the *Sgsf* sgRNA line, each individual offspring male fly was selected to cross with double balancer (*TM3.Sb/TM6.Tb*) flies to establish balanced lines (Kondo and Ueda, 2013). Genomic PCR products using the specific primers covering the mutant sites were cloned into a T-simple vector for further sequencing. The sequencing results showed that two short DNA regions within the open reading frame (ORF) of the *Sgsf* gene were successfully deleted, leading to a frameshift mutation and early termination of translation (Figure S3A).

To generate *UAS-Sgsf-3×HA* transgenic flies, the ORF of the *Sgsf* gene fused to a 3×HA tag at the carboxy-terminus was synthesized by TSINGKE Biological Technology and cloned into the pEASY-Blunt Zero vector. After enzyme digestion and ligation, the *Sgsf-3×HA* sequence was then subcloned into the pUAST plasmid. $Sgsf^{\Delta}$*-3×HA* with a deletion of the signal peptide sequence was amplified from the pEASY-Blunt Zero-*Sgsf*-3×HA plasmid. The pUAST plasmid has been sequenced and confirmed before injection and after generation of transgenic flies. According to the transposable elements in the pUAST plasmid, the *Sgsf-3×HA* and $Sgsf^{\Delta}$*-3×HA* genes were inserted at the attP site of the 25C6 locus on chromosome 2.

To generate transgenic *UAS* fly lines for RNAi-mediated knockdown of the *Sgsf* gene, short hairpins (21 nt) targeting the *Sgsf* gene were designed at an online website (http://biodev.cea.fr/DSIR/DSIR.html). The hairpin sequences were cloned into a VALIUM20 vector and the vectors were then microinjected into *Drosophila* embryos as previously described (Ni et al., 2008, 2009, 2011). The vector has been sequenced and confirmed before injection and after generation of transgenic flies.

### Size and weight measurement

Approximately six fertilized female flies were allowed to lay eggs at 25°C for 6 h in a vial with standard food, and the hatched larvae were moved to a new vial. Approximately 20 male larvae of each genotype at the third larval instar were collected and moved to a new vial for further investigation. After photographing using a Leica M165 FC, the pupal volume was measured using ImageJ and further calculated using the formula $(4/3)\ \pi(L/2)\ (W/2)^2$ (L, length; W, width). For organ size measurement, images of larval salivary gland, wing disc, fat body, and brain were captured by confocal microscopy (Zeiss LSM 880) and the size was analyzed by ImageJ. For measurement of the weight of adult flies, 20 adult flies of each sex were weighed by an electronic microbalance (Garelli et al., 2012; Meschi et al., 2019). Images of the adult wing were captured using a Leica M165 FC, and the size was measured using ImageJ as described previously (Redhai et al., 2020).

### Hemolymph sample preparation and LC-MS/MS analysis

*Drosophila* larvae at 120 h AEL were rinsed with PBS buffer and dried with tissue paper. Then, total hemolymph of 100 larvae was collected by tearing their integument carefully in 70 μL PBS buffer containing 1 mM proteinase inhibitor cocktail (Sigma). After centrifugation, the cell-free supernatants were collected for western blotting. SDS-PAGE was performed on 10% concentration gels. For proteomic analysis, the hemolymph from approximately 100 larvae at 120 h AEL was collected, and the cell-free supernatants after centrifugation were used to perform proteomic analysis using liquid chromatography-tandem mass spectrometry (LC-MS/MS). The proteomic data have been deposited to the ProteomeXchange datasets (Identifier: PXD026372). The signal peptide of selected proteins were in silico predicted using online SignalP-5.0 program.

### Developmental timing

Approximately six fertilized female flies were allowed to lay eggs at 25°C for 6 h in a vial with standard food, and at 48 h AEL, approximately 40 larvae were moved into a new vial containing standard food. Most larvae at 120 h AEL were still feeding. The pupariation rate was recorded every 8 h until all larvae developed into pupae.

### Measurement of feeding and digestion abilities

Blue dye food consisting of bromophenol blue (BPB) sodium salt (0.5% w/v, Sigma) in standard food was used to test larval feeding and digestion abilities. The larvae at 48 h AEL were transferred into prepared blue dye food. After feeding for 45 min, a portion of larvae containing blue dye food in their guts were photographed by Leica M165FC for feeding ability analysis. The remaining larvae were transferred into a new vial containing agar food without any nutrients, and the time at which the blue color in the larval gut disappeared was recorded for the analysis of the digestion ability (Redhai et al., 2020).

To avoid the possibility that food conditions associated with salivary gland ablation are responsible for the effects of the ablation on larval development, we pre-conditioned the food. In brief, ten GFP-labeled larvae (*If/Cyo-GFP*) at 72 h AEL were transferred into a vial. After 24 h when the food became soft and wet, 20 salivary gland-ablated larvae at 48 h AEL were transferred to this vial for rearing. The final pupal volume was recorded and analyzed.

### Semiquantitative RT-PCR and quantitative RT-PCR (RT-qPCR)

Total RNA was extracted from *Drosophila* larval tissues by using TRIzol reagent (Invitrogen). According to the manufacturer's protocol for EasyScript One-step gDNA Removal and cDNA Synthesis Super Mix Kits (TransGen), 1 μg of total RNA was used for cDNA synthesis. Gel electrophoresis-based semiquantitative RT-PCR examination was used to identify the genes that were specifically expressed in salivary glands. In addition, RT-qPCR was performed with NovoStart® SYBR qPCR SuperMix Plus (Novoprotein) by using a 7500 Fast Real-Time PCR System (Applied Biosystems). The *ribosomal protein 49* (*Rp49*) gene was used as the internal control. The relative mRNA expression levels in RT-qPCR analysis were calculated using the $2^{-\Delta\Delta CT}$ method. All experiments were independently performed with three biological replicates. All primers used for semiquantitative RT-PCR and RT-qPCR are listed in Table S2.

### Western blotting

Total proteins were isolated from *Drosophila* tissues and S2 cells using NP-40 lysis buffer (Beyotime) containing 1 mM proteinase inhibitor cocktail (Sigma). Protein samples were prepared according to the procedure as described above. The antibodies used in the experiments include: rabbit anti-phospho-Akt (1:1,000; Cell Signaling Technology), rabbit anti-phospho-S6K (1:1,000; Cell Signaling Technology), rabbit anti-phospho-4E-BP (1:1,000; Cell Signaling Technology), rabbit anti-HA tag (1:1,000; Cell Signaling Technology), rabbit anti-Sgsf (1:2,000; Zoonbio Biotechnology), rabbit anti-Dilp2 (1:1,000; Zoonbio Biotechnology), and mouse anti-tubulin (1:10,000; Beyotime). The secondary antibodies were HRP-conjugated goat anti-rabbit (1:10,000; Beyotime) and goat anti-mouse (1:10,000; Beyotime). Coomassie staining-based total proteins were used as the loading control in analyzing the proteins from the hemolymph (Villoria et al., 2017). Quantitative analysis of western blotting data was performed using ImageJ.

### Immunostaining

*Drosophila* larval tissues at different developmental stages were dissected in PBS and fixed with 4% paraformaldehyde for 30 min at room temperature. After washing three times with PBST buffer (1×PBS including 0.3% Triton X-100), the samples were incubated with primary antibodies at 4°C overnight. The following primary antibodies were used: rabbit anti-Sgsf (1:1,000; Zoonbio Biotechnology) and rabbit anti-Dilp2 (1:500; Zoonbio Biotechnology). After washing in PBST buffer, the samples were incubated with goat anti-rabbit Alexa Fluor 594 (1:1,000; Life Technologies) for 1 h at room temperature. The cell membrane and nucleus were visualized with Alexa Fluor 488-phalloidin (1:500; Invitrogen) and DAPI (1:1,000; Thermo Fisher Scientific), respectively. After washing in PBS buffer, the samples were mounted in Vectashield mounting buffer. The fluorescence signals were captured by confocal microscopy (Zeiss LSM 880). A confocal z stack of Dilp2 signaling in larval brain IPCs was obtained by using a 1 μm step size with identical laser power and scan settings (Geminard et al., 2009). The fluorescence intensity was calculated with ImageJ as described previously (Yang et al., 2021).

### Immunoprecipitation

Immunoprecipitation experiments were used to examine the secretion ability of Sgsf protein in *Drosophila* S2 cells. The ORFs of *Sgsf* and mutated *Sgsf* (*Sgsf*$^{\Delta}$) lacking a signal peptide were separately subcloned into the pMT-V5/HisA vector and were then used for an overexpression analysis in *Drosophila* S2 cells after a sequencing confirmation. At 48 h after transient transfection of the recombinant vectors in S2 cells followed by induction with 500 μM CuSO4, the cells and cell medium were separately collected. The cells were lysed in NP-40 lysis buffer (Beyotime) containing 1 mM protease inhibitor cocktail (Sigma) on ice for 10 min. A cell medium-based immunoprecipitation assay was performed as previously reported (Qian et al., 2020). Briefly, cell medium was incubated with anti-His tag antibody (Beyotime) crosslinked with protein A/G magnetic Dynabeads (Invitrogen) in buffer containing 1 mM protease inhibitor cocktail (Sigma) under gentle rotation at 4°C for 6 h. After washing with NP-40 lysis buffer, the beads were eluted with SDT buffer (100 mM Tris/HCl pH 7.4, 4% SDS) to capture the target proteins. Equal amounts of proteins from cells as input or from immunoprecipitated products were further subjected to western blotting.

### *Ex vivo* brain culture

The brains were dissected from *Drosophila* larvae at 120 h AEL and then transferred to a microfuge tube containing 50 μL of Schneider medium with 10% FBS. Coincubation experiments were performed by adding 10 μL of hemolymph collected from either WT or *Sgsf*$^{-/-}$ larvae at 120 h AEL and incubating for 12 h at room temperature. In addition, the *ex vivo* cultured brains were incubated with 2 μg of purified recombinant Sgsf protein for 12 h at room temperature. After washing three times with PBST buffer (1×PBS including 0.3% Triton X-100), brains were fixed with 4% paraformaldehyde for 30 min at room temperature and then stained with specific anti-Dilp2 antibody.

## QUANTIFICATION AND STATISTICAL ANALYSIS

Data are presented as the mean ± SE of three independent biological replicates. Statistical significance between two groups was determined using an unpaired two-tailed Student's t-test in the GraphPad software and denoted as follows: *p <0.05 and **p <0.01. The significant difference among more than two groups was analyzed using one-way ANOVA followed by Tukey test in the SPSS software. Different letters in the figures indicate a significant difference (p <0.05). All of the statistical details of experiments can be found in the figure legends.

**Cell Reports, Volume *38***

## Supplemental information

# A salivary gland-secreted peptide regulates insect systemic growth

**Zheng Li, Wenliang Qian, Wei Song, Tujing Zhao, Yan Yang, Weina Wang, Ling Wei, Dongchao Zhao, Yaoyao Li, Norbert Perrimon, Qingyou Xia, and Daojun Cheng**

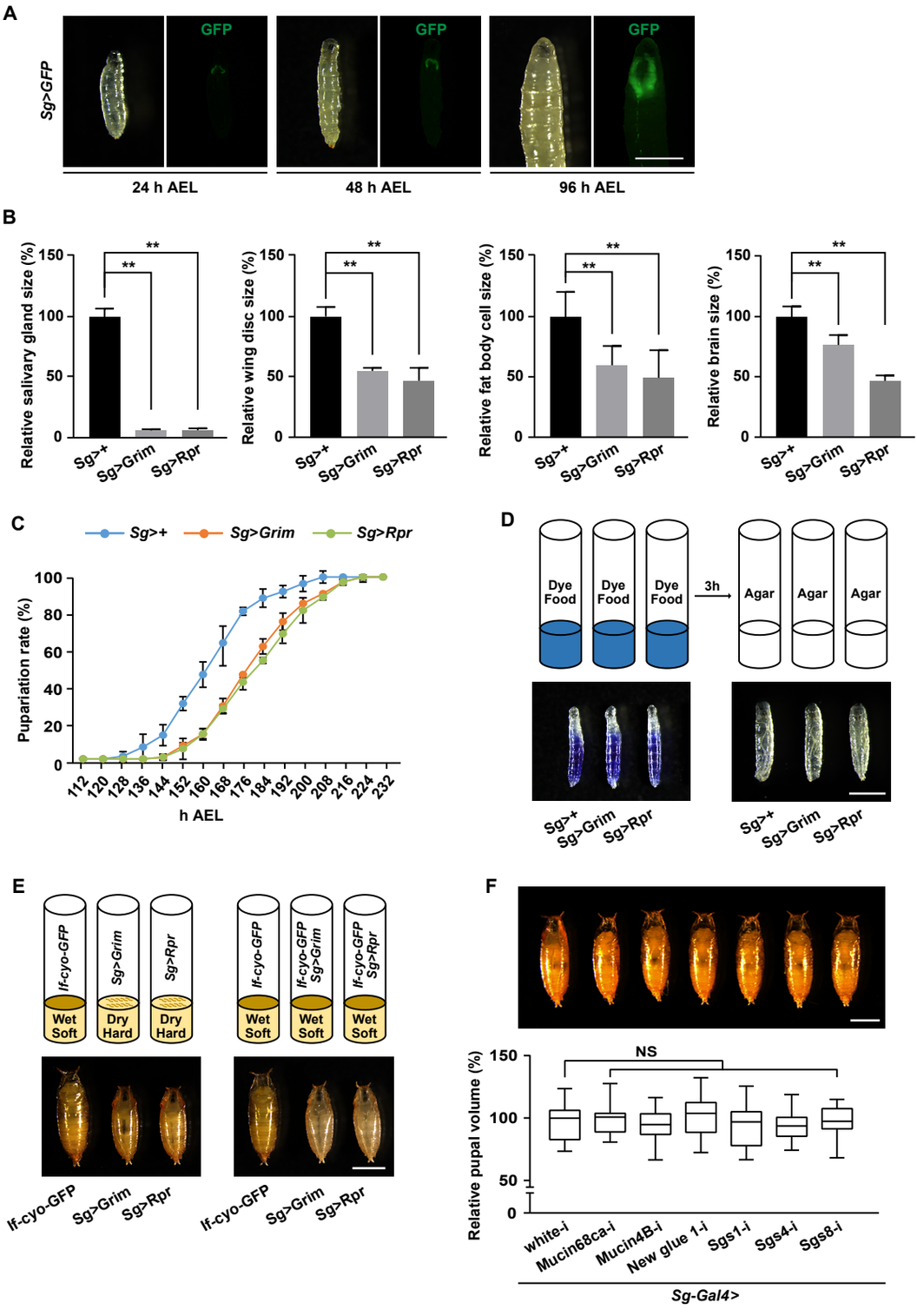


**Figure S1. Effects of salivary gland ablation on developmental timing as well as food digestion and effects of salivary gland-specific knockdown of either *Mucin* or *Glue* genes. Related to Figure 1.**

**(A)** The specificity of the *Sg-Gal4* driver in the salivary gland is confirmed using *Sg-Gal4* to drive *UAS-GFP* expression. Scale bar, 1 mm. **(B)** Quantitative analysis of the size of larval organs at 120 h AEL, including salivary gland, wing disc, fat body cells and brain. **(C)** Ablation of salivary glands causes pupariation delay. AEL, after egg laying. **(D-E)** Deficiency in systemic growth caused by the ablation of salivary glands is not due to the food condition or digestion ability. Scale bar, 1 mm. **(F)** RNAi-mediated salivary gland-specific knockdown of *Mucin* or *Glue* genes does not affect pupal volume, suggesting that salivary gland ablation-induced growth deficiency is not due to exocrine functions of the salivary glands. Scale bar, 1 mm. All experiments were conducted with three biological replicates. Data are presented as the mean ± SE (error bars). For the significance test: $^{**}P < 0.01$ versus the control. NS means no significant difference.

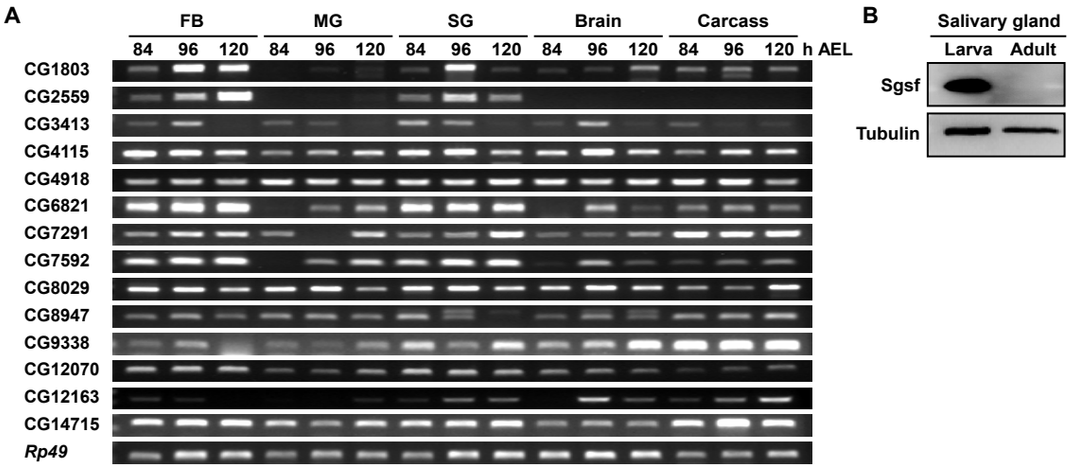
A
FB
MG
SG
Brain
Carcass
84 96 120 84 96 120 84 96 120 84 96 120 84 96 120 h AEL
CG1803
CG2559
CG3413
CG4115
CG4918
CG6821
CG7291
CG7592
CG8029
CG8947
CG9338
CG12070
CG12163
CG14715
Rp49
B
Salivary gland
Larva Adult
Sgsf
Tubulin

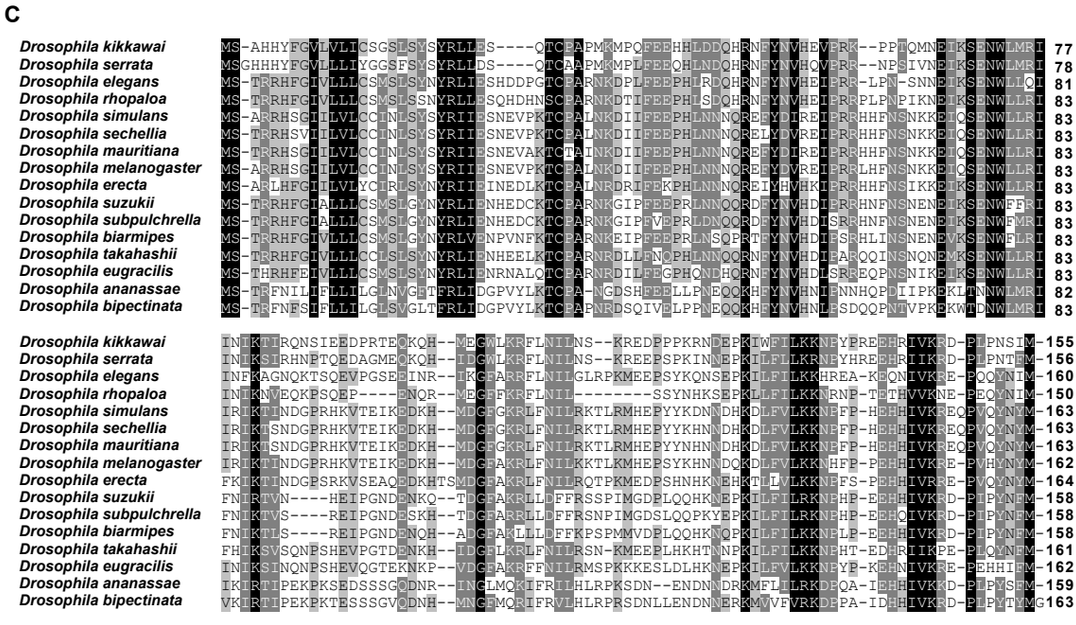
C
Drosophila kikkawai
Drosophila serrata
Drosophila elegans
Drosophila rhopaloa
Drosophila simulans
Drosophila sechellia
Drosophila mauritiana
Drosophila melanogaster
Drosophila erecta
Drosophila suzukii
Drosophila subpulchrella
Drosophila biarmipes
Drosophila takahashii
Drosophila eugracilis
Drosophila ananassae
Drosophila bipectinata

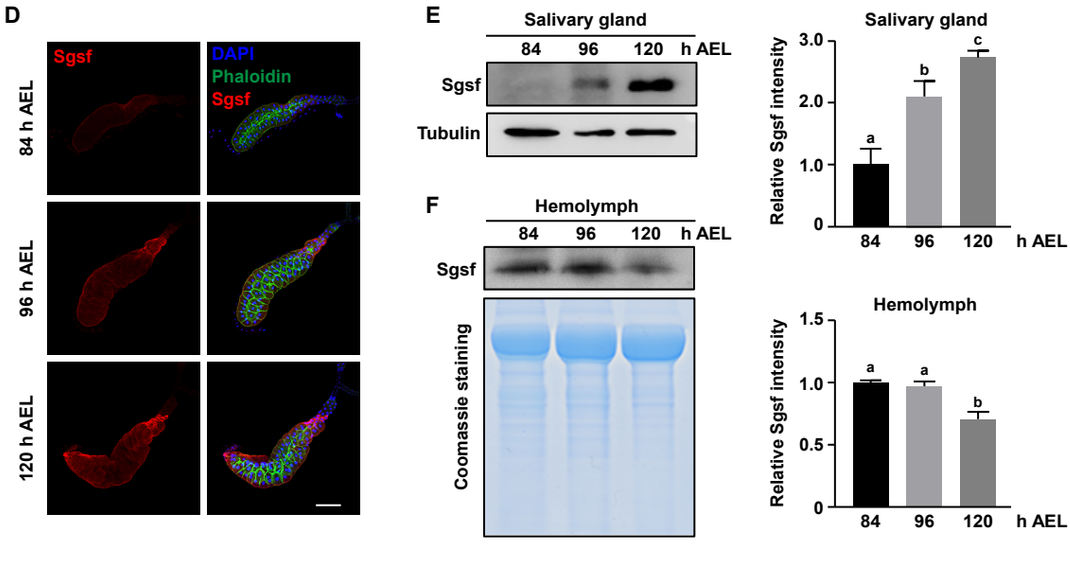
D
Sgsf
DAPI
Phaloidin
Sgsf
84 h AEL
96 h AEL
120 h AEL
E
Salivary gland
84 96 120 h AEL
Sgsf
Tubulin
Salivary gland
Relative Sgsf intensity
3.0
2.0
1.0
0
a
b
c
84 96 120 h AEL
F
Hemolymph
84 96 120 h AEL
Sgsf
Coomassie staining
Hemolymph
Relative Sgsf intensity
1.5
1.0
0.5
0
a
a
b
84 96 120 h AEL

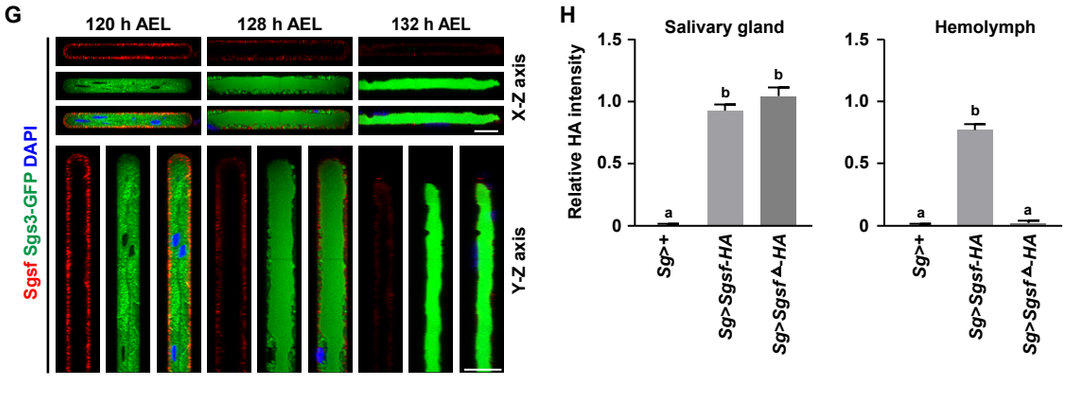
G
120 h AEL
128 h AEL
132 h AEL
X-Z axis
Y-Z axis
Sgsf Sgs3-GFP DAPI
H
Salivary gland
Relative HA intensity
1.5
1.0
0.5
0
a
b
b
Sg>+
Sg>Sgsf-HA
Sg>Sgsf Δ-HA
Hemolymph
1.5
1.0
0.5
0
a
b
a
Sg>+
Sg>Sgsf-HA
Sg>Sgsf Δ-HA

**Figure S2. Expression profile and localization of Sgsf in salivary glands. Related to Figure 2 and STAR Methods.**

**(A)** Semiquantitative RT-PCR examination of the 15 candidate genes that were identified from proteome analysis. **(B)** Sgsf is expressed in salivary glands during the last larval instar but not in adults. **(C)** The orthologs of *Drosophila melanogaster* Sgsf in other *Drosophila* species. **(D-F)** Immunostaining and western blotting determine the level of Sgsf protein in salivary glands and hemolymph during the L3 stage. Tubulin protein and Coomassie staining of total proteins were used as the loading controls for salivary glands and hemolymph, respectively. Scale bar, 200 μm; AEL, after egg laying. **(G)** Sgsf protein is not located in the lumen, which is marked by glue protein Sgs3 during larval-pupal transition. Scale bar, 50 μm. **(H)** Quantitative analysis of secretion ability of Sgsf proteins in *Drosophila* larvae. All experiments were conducted with three biological replicates. Data are presented as the mean ± SE (error bars). Different letters above bars denote significant difference ($P < 0.05$).

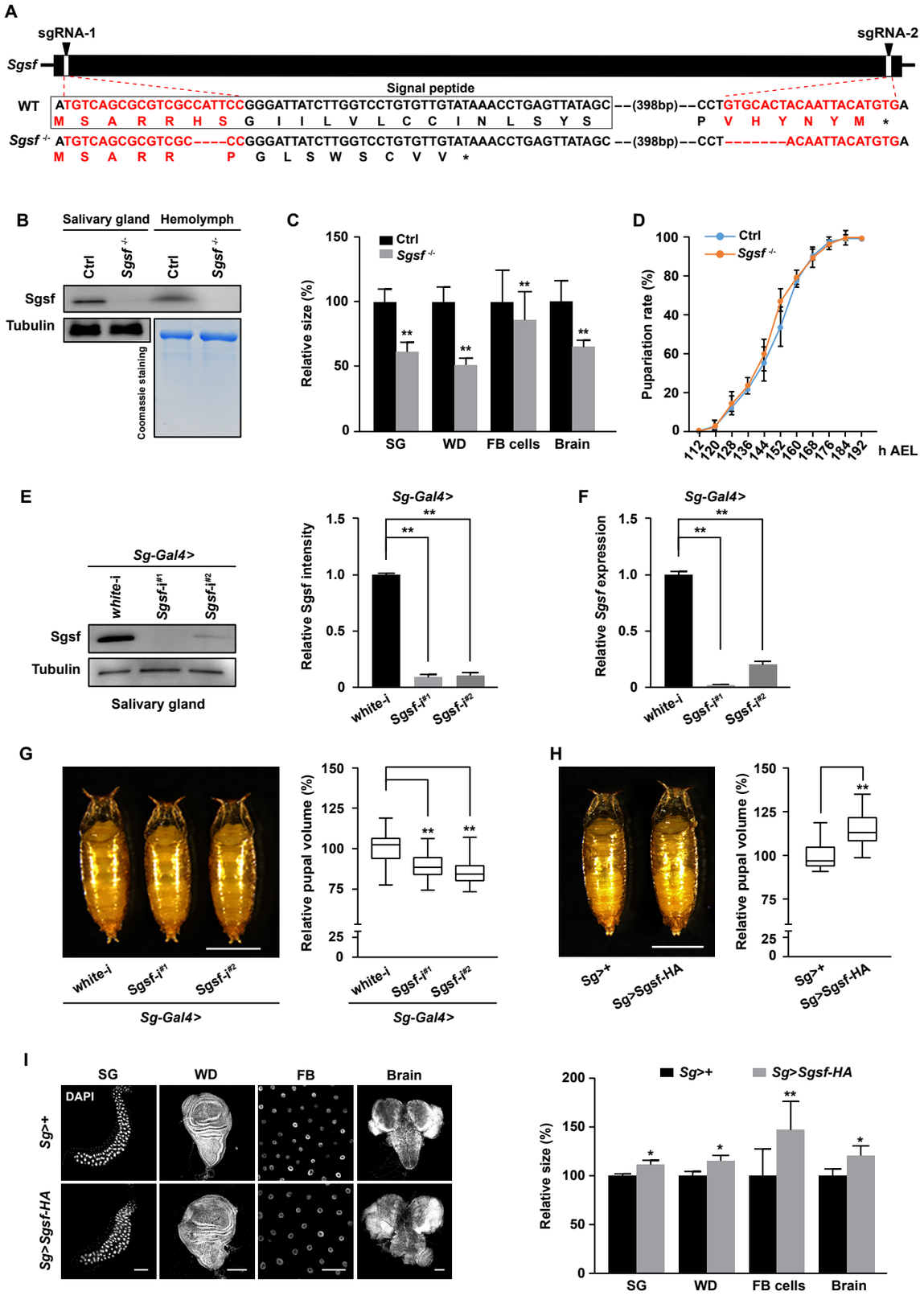


**Figure S3. Effects of Sgsf expression changes on larval systemic growth. Related to Figures 3 and 4.**

**(A)** An 11 base pair deletion in the *Sgsf* gene generated using the CRISPR/Cas9 system causes early termination of translation. The symbol "*" indicates the termination codon. **(B)** Western blotting shows that Sgsf cannot be detected in salivary glands and in the hemolymph of *Sgsf* homozygous mutant larvae. Tubulin and Coomassie staining of total proteins were used as the loading controls for salivary glands and hemolymph, respectively. **(C)** Quantitative analysis of *Sgsf* knockout-induced organ size changes at 120 h AEL. **(D)** *Sgsf* knockout does not affect pupariation time. **(E-G)** Two RNAi lines targeting different genomic regions of the *Sgsf* gene were used to specifically downregulate *Sgsf* expression in salivary glands. Both RNAi lines efficiently downregulate *Sgsf* expression (E-F). SG-specific *Sgsf* knockdown decreases pupal volume (G). *white* RNAi was used as the control. Scale bar, 1 mm. **(H-I)** *Sgsf* overexpression in the salivary gland promotes larval growth and increases the pupal volume and the size of larval organs at 120 h AEL. Scale bar for pupa, 1 mm; scale bar for salivary gland (SG) and wing disc (WD), 200 μm; scale bar for fat body (FB) and brain, 100 μm. AEL, after egg laying. All experiments were conducted with three biological replicates. Data are presented as the mean ± SE (error bars). For the significance test: $*P < 0.05$ and $**P < 0.01$ versus the control.

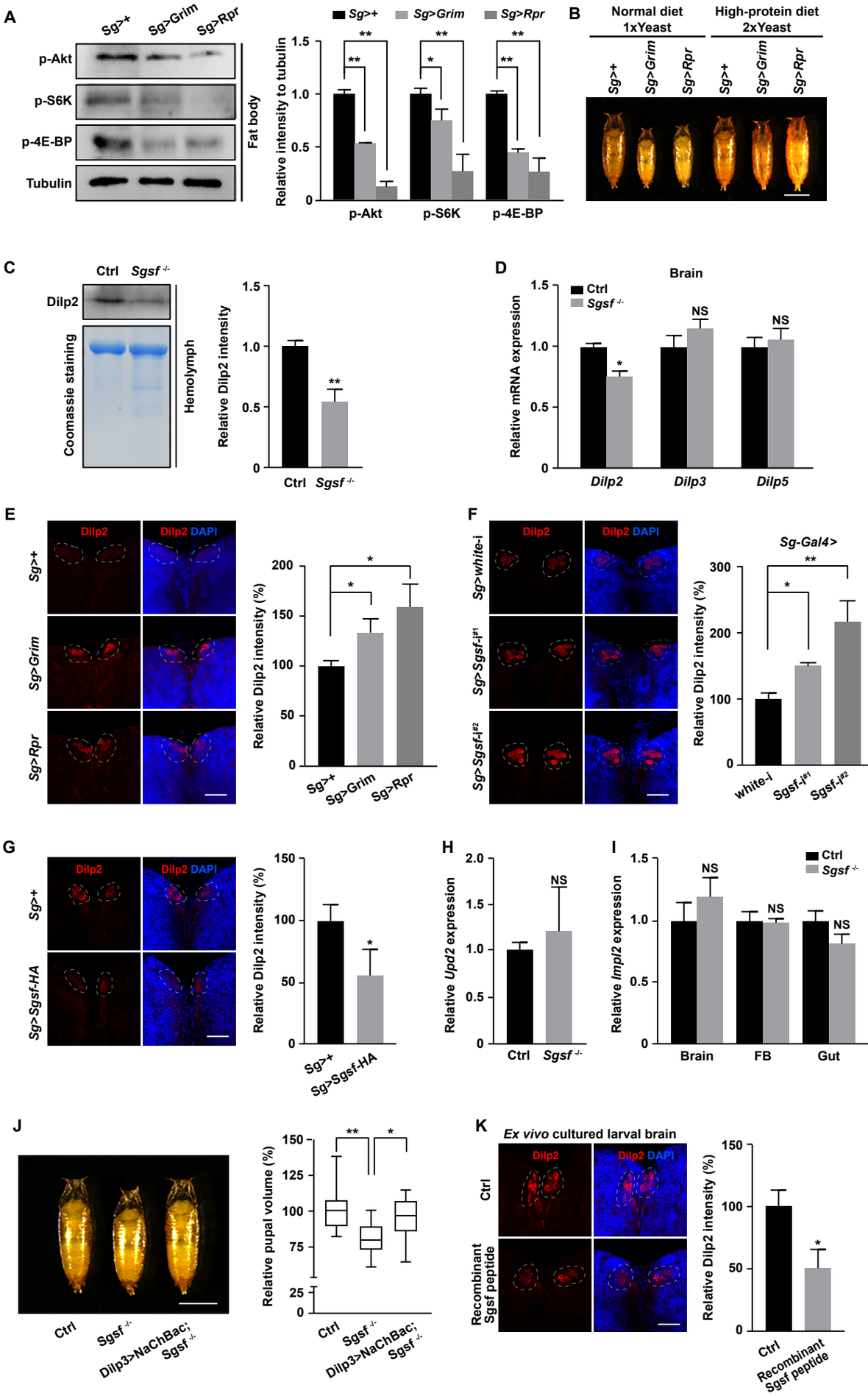
A
Sg>+
Sg>Grim
Sg>Rpr
p-Akt
p-S6K
p-4E-BP
Tubulin
Fat body
Sg>+
Sg>Grim
Sg>Rpr
Relative intensity to tubulin
p-Akt
p-S6K
p-4E-BP
B
Normal diet
1xYeast
High-protein diet
2xYeast
Sg>+
Sg>Grim
Sg>Rpr
C
Ctrl
Sgsf -/-
Dilp2
Coomassie staining
Hemolymph
Relative Dilp2 intensity
D
Brain
Ctrl
Sgsf -/-
Relative mRNA expression
NS
Dilp2
Dilp3
Dilp5
E
Dilp2
Dilp2 DAPI
Sg>+
Sg>Grim
Sg>Rpr
Relative Dilp2 intensity (%)
F
Sg>white-i
Sg>Sgsf-i#1
Sg>Sgsf-i#2
Sg-Gal4>
white-i
Sgsf-i#1
Sgsf-i#2
G
Sg>+
Sg>Sgsf-HA
H
Relative Upd2 expression
I
Relative Impl2 expression
Brain
FB
Gut
J
Ctrl
Sgsf -/-
Dilp3>NaChBac; Sgsf -/-
Relative pupal volume (%)
K
Ex vivo cultured larval brain
Ctrl
Recombinant Sgsf peptide
L
Tub-Gal80ts; Fkh-Gal4>
white-i
EcR-i
Relative pupal volume (%)
M
Relative Sgsf expression
N
Sgsf
Relative Sgsf intensity

**Figure S4. Sgsf could regulate Dilp2 secretion from the IPCs, and the expression and secretion of Sgsf is modulated by ecdysone signaling. Related to Figure 4.**

**(A)** Effects of salivary gland ablation on IIS/mTOR signaling in fat body at 120 h AEL. **(B)** Feeding larvae with high-protein food can rescue the pupal volume decrease induced by salivary gland ablation. Scale bar, 1 mm. **(C)** The Dilp2 protein level in the hemolymph of *Sgsf* $^{-/-}$ larvae is decreased compared to that of the control. Coomassie staining of total proteins was used as a loading control. **(D)** RT-qPCR analysis shows that compared to the control, *Dilp2* mRNA, but not *Dilp3* and *Dilp5* mRNAs, is weakly reduced in the brains of *Sgsf* $^{-/-}$ larvae at 120 h AEL. **(E)** Immunostaining analysis shows an accumulation of Dilp2 in brain IPCs following salivary gland ablation. Scale bar, 50 μm. **(F)** SG-specific *Sgsf* knockdown causes Dilp2 accumulation in brain IPCs. Scale bar, 50 μm. **(G)** *Sgsf* overexpression in salivary glands increases Dilp2 secretion from the IPCs. Scale bar, 50 μm. **(H-I)** *Sgsf* knockout has no effect on *Upd2* expression in the fat body (H) or *Impl2* expression in multiple tissues (I) at 120 h AEL. FB, fat body. **(J)** Enhanced expression of *NaChBac* in the IPCs rescues the pupal volume associated with *Sgsf* knockout. Scale bar, 1 mm. **(K)** Recombinant Sgsf proteins promote Dilp2 secretion from ex vivo cultured brain. Scale bar, 50 μm. **(L-M)** SG-specific knockdown of the ecdysone receptor gene *EcR* at the early L3 stage decreases pupal volume (L) and *Sgsf* mRNA expression (M). **(N)** SG-specific knockdown of *EcR* at the late L3 stage promotes Sgsf secretion into the hemolymph. All experiments were conducted with three biological replicates. Data are presented as the mean ± SE (error bars). For the significance test: $*P < 0.05$ and $**P < 0.01$ versus the control; NS means no significant difference; AEL, after egg laying.

**Table S2 The primers used in this study. Related to STAR Methods.**

| Primer name | Primer sequence |
|---|---|
| **RT-qPCR and RT-PCR ananlysis** | |
| Sgsf-F | 5’ GGGATTATCTTGGTCCTGTGTTG 3’ |
| Sgsf-R | 5’ TATTTCTGTGACTTTATGTCTCGG 3’ |
| Dilp2-F | 5’ AGCAAGCCTTTGTCCTTCATCTC 3’ |
| Dilp2-R | 5’ ACACCATACTCAGCACCTCGTTG 3’ |
| Dilp3-F | 5’ TGTGTGTATGGCTTCAACGCAATG 3’ |
| Dilp3-R | 5’ CACTCAACAGTCTTTCCAGCAGGG 3’ |
| Dilp5-F | 5’ GAGGCACCTTGGGCCTATTC 3’ |
| Dilp5-R | 5’ CATGTGGTGAGATTCGGAGC 3’ |
| Impl2-F | 5’ AAGAGCCGTGGACCTGGTA 3’ |
| Impl2-R | 5’ TTGGTGAACTTGAGCCAGTCG 3’ |
| Upd2-F | 5’ CGGAACATCACGATGAGCGAAT 3’ |
| Upd2-R | 5’ TCGGCAGGAACTTGTACTCG 3’ |
| CG1803-F | 5’ AGTGTGCCTTTTCGGCCTAA 3’ |
| CG1803-R | 5’ CTCGTCCCATGCCAGTCCA 3’ |
| CG2559-F | 5’ ATGGCATACGGATACGGTAAGAC 3’ |
| CG2559-R | 5’ CGATAGCTGTAGCCAATGCC 3’ |
| CG3413-F | 5’ GGACAAGCTGAGGAAACTGC 3’ |
| CG3413-R | 5’ GCGAACCTTCTTAGCAGTGG 3’ |
| CG4115-F | 5’ CATTATCGCCGGAGTGTGC 3’ |
| CG4115-R | 5’ TGCTTGATCCACTCGTTCTC 3’ |
| CG4918-F | 5’ ATGCGTTACGTGGCTGCTTAC 3’ |
| CG4918-R | 5’ GAAGAGAGCGAAGCCCATG 3’ |
| CG6821-F | 5’ CCCGCCTTAACCACAAACC 3’ |
| CG6821-R | 5’ CGAATGGCGAGACAAAGAAGT 3’ |
| CG7291-F | 5’ GCTGAGGTACGCGGTAATTG 3’ |
| CG7291-R | 5’ ATCTCGACGCAGATGATGTCC 3’ |
| CG7592-F | 5’ ATCGTTCTCCTATTGGGTCTGG 3’ |
| CG7592-R | 5’ GCTGGATGTGGATCTTGTGG 3’ |
| CG8029-F | 5’ GATTGCGTTGTGCGTCATTG 3’ |
| CG8029-R | 5’ TTGGTGAGCTTGAGGTCGGT 3’ |
| CG8947-F | 5’ GATTGCGGAACCCTTCTACG 3’ |
| CG8947-R | 5’ GCCTTGTCCACATGCTCATC 3’ |
| CG9338-F | 5’ ATCTTGGCTCTCACCGTCTTG 3’ |
| CG9338-R | 5’ CCAAAGTAGCAGGACCTCACG 3’ |
| CG12070-F | 5’ GCTAATCCCGGAGCTTTGGT 3’ |
| CG12070-R | 5’ TGTCGATCAGCTCATTGGAA 3’ |
| CG12163-F | 5’ TGCGCTATGAGATCCTGCTA 3’ |
| CG12163-R | 5’ GACCTCCTCTTCGTGCTTGT 3’ |
| CG14715-F | 5’ CAGCGATCCGAAAGTGAAG 3’ |
| CG14715-R | 5’ GAAGACGAGCACCGCATTG 3’ |
| Rp49-F | 5’ GACAGTATCTGATGCCCAACA 3’ |
| Rp49-R | 5’ CTTCTTGGAGGAGACGCCGT 3’ |
| **Overexpression in S2 cells** | |
| Sgsf-OE-F | 5’ CCGGAATTCATGTCAGCGCGTCGCCAT 3’ |
| Sgsf-OE-R | 5’ CCGCTCGAGCATGTAATTGTAGTGCACAGGT 3’ |
| Sgsf$^{\Delta}$-OE-F | 5’ CCGGAATTCATGTACAGGATCATAGAAAG 3’ |
| Sgsf$^{\Delta}$-OE-R | 5’ CCGCTCGAGCATGTAATTGTAGTGCACAGGT 3’ |
| **sgRNA for *Sgsf* knockout** | |
| Sgsf-sgRNA-1-F | 5’ TTCGTGTCAGCGCGTCGCCATTCC 3’ |
| Sgsf-sgRNA-1-R | 5’ AAACGGAATGGCGACGCGCTGACA 3’ |
| Sgsf-sgRNA-2-F | 5’ TTCGGTGCACTACAATTACATGTG 3’ |
| Sgsf-sgRNA-2-R | 5’ AAACCACATGTAATTGTAGTGCAC 3’ |
| **Transgenic fly construction** | |
| Sgsf$^{\Delta}$-T-F | 5’ CATGAATTCCGGCCAAGGGCCAATT 3’ |
| Sgsf$^{\Delta}$-T-R | 5’ TACAGGATCATAGAAAGCAATG 3’ |
| shRNA-Sgsf-1-F | 5’ ctagcagtAACGATGGACCGAGACATAAAtagttatattcaagcataTTTATGTCTCGGTCCATCGTTgcg 3’ |
| shRNA-Sgsf-1-R | 5’ aattcgcAACGATGGACCGAGACATAAAtatgcttgaatataactaTTTATGTCTCGGTCCATCGTTactg 3’ |
| shRNA-Sgsf-2-F | 5’ ctagcagtCCGGCTCTAAATAAGGATATAtagttatattcaagcataTATATCCTTATTTAGAGCCGGgcg 3’ |
| shRNA-Sgsf-2-R | 5’ aattcgcCCGGCTCTAAATAAGGATATAtatgcttgaatataactaTATATCCTTATTTAGAGCCGGactg 3’ |
| **Knockout efficiency analysis** | |
| Sgsf-K-F | 5’ TGGTCTCAAGTTCAAGGTTTCATA 3’ |
| Sgsf-K-R | 5’ CTATGTGAGACTTTTGATAAGGGTG 3’ |

Note: F, forward primer; R, reverse primer.